ELSEVIER

Journal of Computational and Applied Mathematics 110 (1999) 241–270

JOURNAL OF COMPUTATIONAL AND APPLIED MATHEMATICS

www.elsevier.nl/locate/cam

Boundary penalty finite element methods for blending surfaces, III. Superconvergence and stability and examples

Zi-Cai Li *, Chia-Shen Chang

Department of Applied Mathematics, National Sun Yat-sen University, Kaohsiung, 80242 Taiwan

Received 15 January 1999; received in revised form 5 May 1999

Abstract

This paper is Part III of the study on blending surfaces by partial differential equations (PDEs). The blending surfaces in three dimensions (3D) are taken into account by three parametric functions, $x(r,t)$, $y(r,t)$ and $z(r,t)$. The boundary penalty techniques are well suited to the complicated tangent (i.e., normal derivative) boundary conditions in engineering blending. By following the previous papers, Parts I and II in Li (J. Comput. Math. 16 (1998) 457–480; J. Comput. Appl. Math. 110 (1999) 155–176) the corresponding theoretical analysis is made to discover that when the penalty power $\sigma = 2$, $\sigma = 3$ (*or* 3.5) and $0 < \sigma \leqslant 1.5$ in the boundary penalty finite element methods (BP-FEMs), optimal convergence rates, superconvergence and optimal numerical stability can be achieved, respectively. Several interesting samples of 3D blending surfaces are provided, to display the remarkable advantages of the proposed approaches in this paper: unique solutions of blending surfaces, optimal blending surfaces in minimum energy, ease in handling the complicated boundary constraint conditions, and less CPU time and computer storage needed. This paper and Li (J. Comput. Math. 16 (1998) 457–480; J. Comput. Appl. Math.) provide a foundation of blending surfaces by PDE solutions, a new trend of computer geometric design.

MSC: 65N10; 65N30

Keywords: Blending surface; Parametric surface; Plate; Mathematical modelling; Biharmonic; Variational equation; Finite element method; Boundary penalty method; Computer geometric design; Superconvergence; Stability

1. Introduction

This paper is a continued study of Li [24,26] on mathematical modelling and numerical techniques for blending surfaces, by partial differential equations (PDEs). In [24], we review the existing blending techniques, such as Foley et al. [16], Hoffmann and Hopcroft [19], Ohkura and Kakazu [32],

* Corresponding author. Fax: +886-7-525-3809.
E-mail address: zcli@math.nsysu.edu.tw (Z.-C. Li)

0377-0427/99/$ - see front matter
PII: S0377-0427(99)00231-9

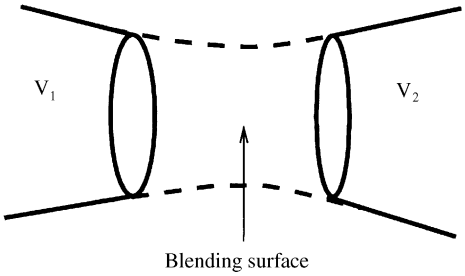

Fig. 1. A blending surface connecting V_1 and V_2 along ∂V_1 and ∂V_2.

Kosters [21], Bajaj and Ihn [3], Choi [9], Farin [14], Fisher [15], Koenderink [20], Nutbourne and Martin [31], Su and Liu [34] and Warren [37]. Only a few [5,6] are involved in differential equations for blending surfaces. In this paper, the real 3D blending surfaces shown in Fig. 1 are considered. A flexibly elastic thin plate is resembled to model the transmitting surfaces for blending two primary surfaces given in Fig. 1. Denote by $x(r,t), y(r,t)$ and $z(r,t)$ the parametric functions of blending surfaces. Then, the solutions $x(r,t), y(r,t)$ and $z(r,t)$ may be governed by a system of the biharmonic equations satisfying the displacement and their derivative boundary conditions. The boundary penalty finite element methods (BF-FEMs) using the piecewise cubic Hermite functions are employed to handle the complicated boundary conditions. In [24], only optimal convergence rates are derived in theory and verified by numerical experiments. Note that the approaches of PDE solutions have many advantages over the existing blending techniques: unique solutions of blending surfaces, optimal blending curves in minimum energy, ease in handling the complicated boundary constraint conditions, and less CPU time and computer storage needed. Toward practical applications, there still exist several important problems of theory and practice to be solved:

(1) Superconvergence of the numerical solutions.
(2) Stability analysis of the BP-FEM because the condition number of the associated matrix resulting from the biharmonic equations is much larger than that resulting from the Poisson equation.
(3) Numerical experiments for producing real blending surfaces in 3D.

To seek solutions to the above problems is the main theme in this paper.

The organization of this paper is as follows. In the next section, the mathematical modelling is addressed to lead to a system of the biharmonic equations of $x(r,t), y(r,t)$ and $z(r,t)$, which are connected only by the boundary tangent conditions. In Section 3, the BP-FEM is developed to handle the boundary constrains and to produce the entire solutions of optimal blending surfaces in the minimum energy. In Section 4, optimal convergence rates, superconvergence and stability analysis are derived together for 3D blending surfaces. The exposition of analysis in Section 4 for real 3D blending surfaces becomes easier by following [26], where only one biharmonic equation is studied. Several blending examples are produced in Section 5 by the numerical techniques, to show the effectiveness of the proposed methods. In the last section, extensions and remarks are provided. The most remarkable advantage of the methods given in this paper and [24,26] is flexible to the complicated blending problems in engineering. This paper and [24,26] provide a foundation of blending surfaces by PDE solutions, a new trend of computer geometric design.

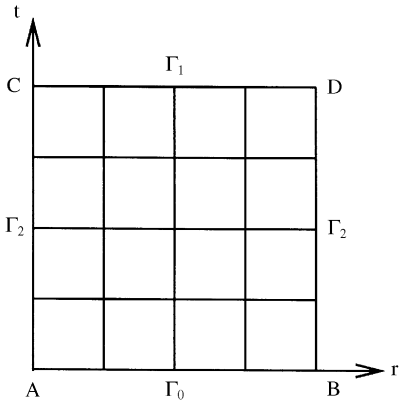

Fig. 2. The solution domain and its partition.

2. Mathematical modelling

Let us consider a real 3D blending surface which is sought to join two given frame bodies V_1 and V_2 at the left boundary ∂V_1 and the right boundary ∂V_2 (see Fig. 1), also see [9,14–16,18]. Suppose that ∂V_1 and ∂V_2 are disjointed to each other. Since the algebraic function $y = f(x, y)$ is difficult to represent the closed surface shown in Fig. 1 (also see [37]), we solicit parametric functions instead. Choose two parameters r and t in a unit solution area $\Omega = \{(r,t), 0 \leqslant r \leqslant 1, 0 \leqslant t \leqslant 1\}$, and use the vector of three parametric functions,

$$U = U(r,t) = (x,y,z)^{\mathrm{T}} = (x(r,t), y(r,t), z(r,t))^{\mathrm{T}}, \quad (r,t) \in \Omega \tag{2.1}$$

to represent the blending surface. Naturally, we denote the boundary of Ω (see Fig. 2) by $\Gamma = \partial\Omega = \Gamma_0 \cup \Gamma_1 \cup \Gamma_2$, where $\Gamma_0 = \overline{AB}$, $\Gamma_1 = \overline{CD}$, and $\Gamma_2 = \overline{AC} \cup \overline{BD}$. Therefore, the displacement and tangent conditions of 3D blending surfaces along the joint boundaries ∂V_1 and ∂V_2 can be written as

$$U|_{\overline{AC}} = U|_{r=0} = U_0, \qquad U|_{\overline{BD}} = U|_{r=1} = U_1 \quad (\text{or } U|_{\Gamma_2} = \bar{U}), \tag{2.2}$$

$$(u_n)_{\overline{AC}} = (u_n)_{r=0} = \alpha_0 U_0', \qquad (u_n)_{\overline{BD}} = (u_n)_{r=1} = \alpha_1 U_1', \tag{2.3}$$

where $U_n = (\partial/\partial n)U$, and n is the outer normal to the boundary $\partial\Omega$. The vectors $U_0, U_1, U_0' (\neq 0)$ and $U_1' (\neq 0)$ are known, but the ratio functions $\alpha_0(t) (\neq 0)$ and $\alpha_1(t) (\neq 0)$ are arbitrary real functions. We may express (2.3) as

$$y_n = b_{10} x_n, \quad z_n = b_{20} x_n \quad \text{on } \overline{AC}, \qquad y_n = b_{11} x_n, \quad z_n = b_{21} x_n \quad \text{on } \overline{BD} \tag{2.4}$$

or simply as

$$y_n = b_1 x_n, \quad z_n = b_2 x_n \quad \text{on } \Gamma_2, \tag{2.5}$$

where b_{10}, b_{20}, b_{11} and b_{21} (or b_1 and b_2) are known and obtained from the ratios of derivatives in (2.3). For the closed surface along direction t, the following periodical conditions on Γ_1 will be satisfied:

$$U(r,0) = U(r,1), \qquad U_t(r,0) = U_t(r,1), \quad 0 \leqslant r \leqslant 1. \tag{2.6}$$

Let $C^k(\Omega)$ denote a space of functions having continuous derivatives of order k. Since functions $x(r,t), y(r,t)$, and $z(r,t) \in C^1(\Omega)$, and the continuity of U and U_n on $\partial\Omega$ is described in (2.2), (2.5) and (2.6), we may assume that the solution $x, y, z (\in C^4(\Omega))$ satisfy the following biharmonic equations which resemble the placements in flexible elastic plates:

$$\Delta^2 U = F \quad \text{where } F = (f_x, f_y, f_z)^{\mathrm{T}}, \tag{2.7}$$

where the Laplace operator $\Delta = (\partial^2/\partial x^2) + (\partial^2/\partial y^2)$, and the biharmonic operator $\Delta^2 = ((\partial^2/\partial x^2) + (\partial^2/\partial y^2))^2$. The functions f_x, f_y, and f_z denote the external loading forces on the thin plate and they can be chosen suitably based on practical experiments and requirements in engineering.

Note that Eq. (2.7), accompanied only with the essential boundary conditions (2.2), (2.3) and (2.6), will lead to many solutions (see [16, p. 486]). We derive in [24] the additional boundary conditions

$$M(U) \cdot B = 0, \tag{2.8}$$

$$P(U(r,0)) + P(U(r,1)) = 0, \qquad M(U(r,0)) + M(U(r,1)) = 0, \quad 0 \leqslant r \leqslant 1, \tag{2.9}$$

where $B = (1, b_1, b_2)^{\mathrm{T}}$ and the notations are

$$M(U) = -\Delta U + (1-\mu)(U_{rr} r_s^2 + 2U_{rt} r_s t_s + U_{tt} t_s^2), \tag{2.10}$$

$$P(U) = \frac{\partial}{\partial n}\Delta U + (1-\mu)\frac{\partial}{\partial s}\{U_{rr} r_n r_s + U_{rt}(r_n t_s + r_s t_n) + U_{tt} t_n t_s\}, \tag{2.11}$$

where r_n, t_n and r_s, t_s are the direction cosines of the outnormal and vectors, respectively.

The boundary conditions (2.8) and (2.9) are called the natural conditions; and Eqs. (2.2), (2.5) and (2.6) are the essential conditions. Both the essential and natural boundary conditions should be implemented to the differential equation (2.7) to yield a unique solution U.

Now we give the variational equations of biharmonic functions (see [11,17]). Denote two spaces H and H_0 of U such that

$$H = \{(x,y,z) \,|\, x, y, z \in H^2(\Omega), \text{ satisfying (2.2), (2.5) and (2.6)}\}, \tag{2.12}$$

$$H_0 = \{(x,y,z) \,|\, x, y, z \in H^2(\Omega), \text{ satisfying } U|_{\Gamma_2} = 0, \text{ (2.5) and (2.6)}\}, \tag{2.13}$$

where $H^2(\Omega)$ is the Sobolev space (see [30]). A solution $U \in H$ can be expressed in a weak form (Galerkin problem)

$$A(U, W) = F(W), \quad \forall W \in H_0, \tag{2.14}$$

where

$$A(U,W) = \int\int_{\Omega} \{\Delta U \cdot \Delta W + (1-\mu)(2U_{rt} \cdot W_{rt} - U_{rr} \cdot W_{tt} - U_{tt} \cdot W_{rr})\} \,\mathrm{d}r\,\mathrm{d}t, \tag{2.15}$$

$$F(U) = \int\int_{\Omega} F \cdot W \,\mathrm{d}r\,\mathrm{d}t, \tag{2.16}$$

and $U_{rr} = \partial^2 U/\partial r^2$, $U_{rt} = \partial^2 U/\partial r \partial t$, $W = (\xi, \eta, \zeta)^{\mathrm{T}}$, and μ is the Poisson ratio satisfying $0 < \mu < \frac{1}{2}$. Also the notation $U \cdot W$ denotes the scalar product of vectors.

Note that Galerkin problem (2.14) requires only the essential boundary conditions, where $x, y, z \in H^2(\Omega)$ are required to be less smooth than $x, y, z \in C^4(\Omega)$ required in (2.7). The true solution U can also be restated as the variational problem:

$$I(U) = \min_{W \in H} I(W), \qquad I(U) = \tfrac{1}{2}A(U,U) - F(U) \tag{2.17}$$

which also indicates the minimal, global energy of the optimal blending surfaces obtained (also see [13]).

3. Boundary penalty finite element methods

To deal with conditions (2.5) and (2.6), a direct treatment is introduced in Li [22] by eliminating some unknowns on the boundary; but the treatment may cause some complexity in programming; we will here follow the penalty techniques described in [23,2,4,33,35,36], to simplify numerical algorithms.

Let the square solution area Ω be divided into small quasi-uniform rectangular elements by the coordinate lines $r = r_i$ and $t = t_j$ (see Figs. 2–4), where

$$\begin{aligned} &0 = r_0 < r_1 < \cdots < r_i < \cdots < r_n = 1, \quad n \geqslant 1, \\ &0 = t_0 < t_1 < \cdots < t_j < \cdots < t_m, \quad m \geqslant 2. \end{aligned} \tag{3.1}$$

Denote the stepsizes $\delta r_i = r_{i+1} - r_i$, $\delta t_j = t_{j+1} - t_j$, and the small rectangular elements $\square_{ij}$ (see Fig. 5(a)) by

$$\square_{i,j} = \{(r,t), r_i \leqslant r \leqslant r_{i+1}, t_j \leqslant t \leqslant t_{j+1}\}. \tag{3.2}$$

For each element node $(i,j) = (r_i, t_j)$, we assign four unknowns, e.g., x_{ij}, $(x_r)_{ij}$, $(x_t)_{ij}$, and $(x_{rt})_{ij}$ of function $x(r,t)$. Also denote the basis functions with the nonzero supports:

$$\phi_{i,\ell} = \phi_\ell\left(\frac{r - r_i}{\delta r_i}\right), \qquad \psi_{i,\ell} = \psi_\ell\left(\frac{r - r_i}{\delta r_i}\right), \quad \ell = 0, 1,$$

$$\phi_{j,\ell} = \phi_\ell\left(\frac{t - t_j}{\delta t_j}\right), \qquad \psi_{j,\ell} = \psi_\ell\left(\frac{t - t_j}{\delta t_j}\right), \quad \ell = 0, 1,$$

where the cubic Hermite functions on $[0,1]$ are (see [7]).

$$\begin{aligned} &\phi_0(r) = 2r^3 - 3r^2 + 1, \qquad \phi_1(r) = -2r^3 + 3r^2, \\ &\psi_0(r) = \phi_2(r) = r^3 - 2r^2 + r, \qquad \psi_1(r) = \phi_3(r) = r^3 - r^2. \end{aligned} \tag{3.3}$$

The following piecewise bi-cubic Hermite polynomials can be formulated for $x_h(r,t)$ in two dimensions:

$$\begin{aligned} x_h(r,t) = \sum_{i=0}^{n-1}\sum_{j=0}^{m-1}\sum_{k,\ell=0}^{1} \{ & x_{i+k,j+\ell}\phi_{i,k}(r)\phi_{j,\ell}(t) + \delta r_i (x_r)_{i+k,j+\ell}\psi_{i,k}(r)\phi_{j,\ell}(t) \\ & + \delta t_j (x_t)_{i+k,j+\ell}\phi_{i,k}(r)\psi_{j,\ell}(t) + \delta r_i \delta t_j (x_{rt})_{i+k,j+\ell}\psi_{i,k}(r)\psi_{j,\ell}(t)\}. \end{aligned} \tag{3.4}$$

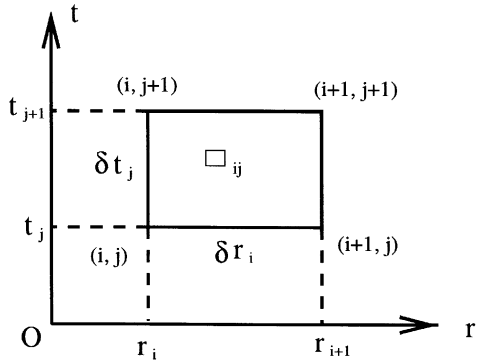

Fig. 3. A rectangular element.

In this paper we also employ the variable transformation as in [26]

$$x^*_{i,j} = x_{i,j}, \quad (x^*_r)_{i,j} = \delta r (x_r)_{i,j}, \quad (x^*_t)_{i,j} = \delta r (x_t)_{i,j}, \quad (x^*_{rt})_{i,j} = \delta r \delta t (x_{rt})_{i,j}, \tag{3.5}$$

where δr and δt are the average meshspacings of δr_i and δt_j given by

$$\delta r = \sum_{i=1}^{n} \frac{\delta r_i}{n}, \qquad \delta t = \sum_{j=1}^{m} \frac{\delta t_j}{m}. \tag{3.6}$$

Hence the admissible functions are expressed as

$$x_h(r,t) = \sum_{i=0}^{n-1} \sum_{j=0}^{m-1} \sum_{k,\ell=0}^{1} \left\{ x^*_{i+k,j+\ell} \phi_{i,k}(r) \phi_{j,\ell}(t) + \left(\frac{\delta r_i}{\delta r} \right) (x^*_r)_{i+k,j+\ell} \psi_{i,k}(r) \phi_{j,\ell}(t) \right.$$
$$\left. + \left(\frac{\delta t_j}{\delta t} \right) (x^*_t)_{i+k,j+\ell} \phi_{i,k}(r) \psi_{j,\ell}(t) + \left(\frac{\delta r_i}{\delta r} \right) \left(\frac{\delta t_j}{\delta t} \right) (x^*_{rt})_{i+k,j+\ell} \psi_{i,k}(r) \psi_{j,\ell}(t) \right\}. \tag{3.7}$$

The admissible functions are then written as

$$U_h = U_h(r,t) = (x_h(r,t), y_h(r,t), z_h(r,t))^{\mathrm{T}}, \tag{3.8}$$

where $y_h(r,t)$ and $z_h(r,t)$ are also defined in (3.4) or (3.7). Obviously, $x_h, y_h, z_h \in H^2(\Omega) \cap C^1(\Omega)$. Define a finite-dimensional collection of the functions as

$$V_h = \{U \text{ as (3.8), satisfying (2.2)}\}, \tag{3.9}$$

$$V_h^0 = \{U \text{ as (3.8), satisfying } U|_{\Gamma_2} = 0\}. \tag{3.10}$$

Conditions in (2.2) still remain in spaces V_h and V_h^0, but neither (2.5) nor (2.6) in V_h and V_h^0. Hence if compared to the functional spaces H and H_0 in (2.12) and (2.13), we can see

$$V_h^0 \not\subset H_0, \quad V_h \not\subset H. \tag{3.11}$$

Therefore, we should invoke the penalty techniques to impose the boundary conditions (2.5) and (2.6). The solution $U_h^* \in V$ can then be obtained from the boundary penalty finite element method (BP-FEM),

$$A_p(U_h^*, W_h) = F_h(W_h), \quad \forall W_h \in V_h^0, \tag{3.12}$$

where

$$F_h(W) = \int\!\!\int_{\Omega} \hat{F} \cdot W \, \mathrm{d}s. \tag{3.13}$$

$\hat{F}$ is the piecewise bilinear and cubic Hermite interpolatory functions of F for optimal rates and superconvergence, respectively, and

$$A_p(U_h, W_h) = A(U_h, W_h) + \bar{D}(U_h, W_h), \tag{3.14}$$

$A(U, W)$ is given in (2.15) already, and h is the maximal length of quasiuniform elements defined by $h = \max_{ij}(\delta r_i, \delta t_j)$. The boundary penalty integrals $\bar{D}(U, W)$ are designed to impose (2.5) and (2.6), given by [24]:

$$\begin{aligned}\bar{D}(U, W) = \frac{P_c}{h^{2\sigma}} \Bigg\{ & \int_{\Gamma_2} (y_n - \bar{b}_1 x_n)(\eta_n - \bar{b}_1 \xi_n) \, \mathrm{d}\ell + \int_{\Gamma_2} (z_n - \bar{b}_2 x_n)(\zeta_n - \bar{b}_2 \xi_n) \, \mathrm{d}\ell \\ & + \int_0^1 (U(r,0) - U(r,1))(W(r,0) - W(r,1)) \, \mathrm{d}r \\ & + \int_0^1 (U_n(r,0) - U_n(r,1))(W_n(r,0) - W_n(r,1)) \, \mathrm{d}r \Bigg\},\end{aligned} \tag{3.15}$$

where $P_c(>0)$ is a bounded positive constant independent of h, and $\sigma(>0)$ is a penalty power. Note that $\bar{b}_i$ used in (3.15) are the piecewise q-order interpolatory polynomials of functions b_i, where $1 \leqslant q \leqslant 3$. When $q = 3$, $\bar{b}_i$ are chosen as the piecewise cubic Hermite interpolants of b_i. By the analysis of Li [24], we need the same penalty factor $P_c/h^{2\sigma}$ used for all boundary conditions of both displacement and derivatives. The exact integrals in $\bar{D}(U, W)$ may also be evaluated directly due to polynomial integrands, or from integration rules with accuracy of order up to $6 + 2q$. In the latter, Gaussian rules are suggested with integration nodes up to $4 + q$. Furthermore, integration rules of order four and six can evaluate exactly integrals $A_h(U_h, W_h)$ and $F_h(U_h)$, respectively (see [12]).

For superconvergence, we will choose the variants of the BP-FEM as follows:

$$\hat{A}_p(\hat{U}_h^*, W_h) = F_h(W_h), \quad \forall W_h \in V_h^0, \tag{3.16}$$

where

$$\hat{A}_p(U, W) = A(U, W) + \hat{D}(U, W), \tag{3.17}$$

$A(U, W)$ and $F_h(W)$ are the same as in (3.12), but $\hat{D}(U, W)$ is defined differently by

$$\begin{aligned}\bar{D}(U, W) = \frac{P_c}{h^{2\sigma}} \Bigg\{ & \widehat{\int_{\Gamma_2}} (y_n - b_1 x_n)(\eta_n - b_1 \xi_n) \, \mathrm{d}\ell + \widehat{\int_{\Gamma_2}} (z_n - b_2 x_n)(\zeta_n - b_2 \xi_n) \, \mathrm{d}\ell \\ & + \widehat{\int_0^1} (U(r,0) - U(r,1))(W(r,0) - W(r,1)) \, \mathrm{d}r \\ & + \widehat{\int_0^1} (U_n(r,0) - U_n(r,1))(W_n(r,0) - W_n(r,1)) \, \mathrm{d}r \Bigg\}.\end{aligned} \tag{3.18}$$

In (3.18) $P_c(>0)$ and $\sigma(>0)$ are also the penalty constant and power independent of h, and the approximate integrals $\widehat{\int_0^1}$ and $\widehat{\int_{\Gamma_2}}$ are evaluated by the following rules:

$$\widehat{\int_0^1} uv\,\mathrm{d}r = \int_0^1 \hat{u}\hat{v}\,\mathrm{d}r = \int_0^1 u_I v_I\,\mathrm{d}r, \tag{3.19}$$

$\hat{u}$ and $\hat{v}$ are the piecewise cubic Hermite interpolants of u and v, respectively, and the integration rule with higher order is needed for $\widehat{\int_{\Gamma_2}}$ given by

$$\widehat{\int_{\Gamma_2}} fg\,\mathrm{d}\ell = \int_{\Gamma_2} \hat{f}\hat{g}\,\mathrm{d}\ell = \int_{\Gamma_2} (\Pi^5 f_I)(\Pi_p^5 g_I)\,\mathrm{d}\ell, \tag{3.20}$$

where $\hat{f}$ (or $\hat{g}$) are the piecewise Hermite interpolant of order 5 of f (or g) on $[t_{2j}, t_{2j+2}]$ using the nodal values $f_{2j}, f_{2j+1}, f_{2j+2}, (\partial f/\partial t)_{2j}, (\partial f/\partial t)_{2j+1}$ and $(\partial f/\partial t)_{2j+2}$. Note that when $f = \eta_n - b_1\xi_n = \eta_r - b_1\xi_r$, the nodal values at $(0, t_j)$ and $(1, t_j)$ on Γ_2 are given by

$$f_j = (\eta_r)_j - (b_1)_j(\xi_r)_j, \qquad \left(\frac{\partial f}{\partial t}\right)_j = (\eta_{rt})_j - ((b_1)_j(\xi_{rt})_j + ((b_1)_t)_j(\xi_r)_j), \quad r = 0, 1. \tag{3.21}$$

The cubic Hermite functions in $[s_i, s_{i+1}]$ with u_i and u_i' are then expressed by

$$u_h(s) = u_i\phi_0\left(\frac{s-s_i}{h_i}\right) + u_{i+1}\phi_1\left(\frac{s-s_i}{h_i}\right) + u_i' h_i\psi_0\left(\frac{s-s_i}{h_i}\right) + u_{i+1}' h_i\psi_1\left(\frac{s-s_i}{h_i}\right) \tag{3.22}$$

and $\phi_k(s)$ and $\psi_k(s)$, $k = 0, 1$ are given in (3.3).

Let $u = u(s)$ in one dimension, and construct the interpolant polynomials $\Pi_{2h}^5 u_I$ of order 5 on $[s_{2i}, s_{2i+2}]$ with the supports, u_{2i}, u_{2i+1}, u_{2i+2}, u_{2i}', u_{2i+1}' and u_{2i+2}'. Below we give an explicit formula for the interpolation $\Pi_{2h}^5\hat{u}_h$ on Γ_2, which is used for the boundary integration in (3.20); and the a posteriori interpolants $\Pi_p^5\tilde{U}_h^*$ over Ω can be obtained by tensor product. Assume that the known solutions and their derivatives are given by

$$\begin{aligned} &\hat{u}_0 = u(0), \qquad \hat{u}_1 = u(1), \qquad \hat{u}_2 = u(2),\\ &\hat{u}_0' = u'(0), \qquad \hat{u}_1' = u'(1), \qquad \hat{u}_2' = u'(2). \end{aligned}$$

Then the Hermite interpolation of order 5 on [0,2] can be obtained from Alkinson [1, p. 160]:

$$P_5(s) = \hat{u}_0 T_0(s) + \hat{u}_1 T_1(s) + \hat{u}_2 T_2(s) + \hat{u}_0' Q_0(s) + \hat{u}_1' Q_1(s) + \hat{u}_2' Q_2(s), \tag{3.23}$$

where

$$\begin{aligned} &T_0(s) = \tfrac{1}{4}(1+3s)(s-1)^2(s-2)^2, \quad T_1(s) = s^2(s-2)^2,\\ &T_2(s) = \tfrac{1}{4}(1-3(s-2))s^2(s-1)^2, \quad Q_0(s) = \tfrac{1}{4}s(s-1)^2(s-2)^2,\\ &Q_1(s) = (s-1)s^2(s-2)^2, \quad Q_2(s) = \tfrac{1}{4}(s-2)s^2(s-1)^2. \end{aligned} \tag{3.24}$$

Let the division number be even, i.e., N is even and $h_{2i} = h_{2i+1}$. Then we may establish the following Hermite interpolation with order 5 on $[s_{2i}, s_{2i+2}]$:

$$\begin{aligned} \Pi_{2h}^5 u_h(s) = {} & x_{2i} T_0\left(\frac{s-s_{2i}}{h_{2i}}\right) + x_{2i+1} T_1\left(\frac{s-s_{2i}}{h_{2i}}\right) + x_{2i+2} T_2\left(\frac{s-s_{2i}}{h_{2i}}\right)\\ & + x_{2i}' h_{2i} Q_0\left(\frac{s-s_{2i}}{h_{2i}}\right) + x_{2i+1}' h_{2i} Q_1\left(\frac{s-s_{2i}}{h_{2i}}\right) + x_{2i+2}' h_{2i} Q_2\left(\frac{s-s_{2i}}{h_{2i}}\right). \end{aligned} \tag{3.25}$$

4. Convergence, Superconvergence and Stability

In this section, we will cite convergence from Li [24], and derive superconvergence and stability for $\mu \in [0, \frac{1}{2})$. Since the analysis on optimal convergence, superconvergence and stability may follow the analysis in [24,26], we only pay attention to different arguments in proof so that all the analysis is condensed into one section.

4.1. Optimal convergence

By the Green theory, we have for $\mu \in [0, \frac{1}{2})$.

$$\int\int_{\Omega} (\Delta^2 U - F) \cdot W \, \mathrm{d}s + \int_{\partial\Omega} P(U) \cdot W \, \mathrm{d}\ell - \int_{\partial\Omega} M(U) \cdot W_n \, \mathrm{d}\ell, \tag{4.1}$$

where $M(U)$ and $P(U)$ are given in (2.10) and (2.11). First denote a norm

$$|\,\|U\|\,| = \{\|U\|^2_{(H^2(\Omega))^3} + \bar{D}(U,U)\}^{1/2}, \tag{4.2}$$

where $\bar{D}(U,U)$ is given in (3.15), using $q-$ $(1 \leqslant q \leqslant 3)$ order interpolatory polynomials $\bar{b}_i$ of b_i. The norm notations are

$$\|U\|_{(H^k(\Omega))^3} = \{\|x\|^2_{H^k(\Omega)} + \|y\|^2_{H^k(\Omega)} + \|z\|^2_{H^k(\Omega)}\}^{1/2}, \tag{4.3}$$

$$|U|_{(H^k(\Omega))^3} = \{|x|^2_{H^k(\Omega)} + |y|^2_{H^k(\Omega)} + |z|^2_{H^k(\Omega)}\}^{1/2} \tag{4.4}$$

and $\|x\|^2_{H^k(\Omega)}$ and $|x|^2_{H^k(\Omega)}$ are the Sobolev norms (see Marti (86)). We have the following lemma.

Lemma 4.1. *Let $\mu \in [0, \frac{1}{2})$, there exist two bounded positive constants C_0 and C_1 independent of h and σ such that*

$$|A_p(W,U)| \leqslant C_1 |\,\|W\|\,| \times |\,\|U\|\,|, \quad W \in H_0 \text{ and } U \in V_h^0 \tag{4.5}$$

and the uniformly V_h^0-elliptic inequality

$$C_0 |\,\|U\|\,|^2 \leqslant A_P(U,U), \quad U \in V_h^0. \tag{4.6}$$

Proof. We have

$$A(U,U) = \mu(U_{rr} + U_{tt})^2 + (1-\mu)(U_{rr}^2 + 2U_{rt}^2 + U_{tt}^2). \tag{4.7}$$

Then when $\mu \in [0, \frac{1}{2})$,

$$A_p(U,U) = A(U,U) + \bar{D}(U,U) \geqslant A(U,U) \geqslant \tfrac{1}{2}|U|_2^2. \tag{4.8}$$

Moreover, when $A_p(U,U) = 0$, then $A(U,U) = 0$ implies $U_{rr} = U_{rt} = U_{tt} = 0$. In this case, U are linear functions. Since $U \in V_h^0$, $U|_{\Gamma_2} = 0$, and then $U \equiv 0$. Therefore, based on the generalized Friedrichs' inequality (see Marti (86, p. 82)) we obtain

$$\|U\|_2^2 \leqslant C_2 \left\{ |U|_2^2 + \int_{\Gamma_2} U^2 \, \mathrm{d}\ell \right\} = C_2 |U|_2^2 \leqslant 2C_2 A_p(U,U), \tag{4.9}$$

where C_2 is also a positive bounded constant. This is (4.6); and the proof for (4.5) is easier. We complete the proof of Lemma 4.1. □

Now let us cite a theorem and a corollary from Li [24].

Theorem 4.2. *Let* $U \in (H^4(\Omega))^3$, $F \in (H^2(\Omega))^3$, $U \in (H^4(\Gamma))^3$, $U_n \in (H^4(\Gamma))^3$, $M(U) \in (H^0(\Gamma))^3$, $P(U) \in (H^0(\Gamma_1))^3$ *and* $B \in (H^{q+1}(\Gamma_2))^2$ *be given. When* $\hat{F}$ *in* (3.13) *is the piecewise bilinear interpolant of* F. *Then for* $\mu \in [0, \frac{1}{2})$, *there exists a bounded constant* C *independent of* h and σ *such that*

$$\begin{aligned} |\,\|U - U_h^*\|\,| \leqslant C\{&h^2(|U|_{(H^4(\Omega))^3} + |F|_{(H^2(\Omega))^3}) + h^\sigma(|M(U)|_{(H^0(\Gamma))^3} + |P(U)|_{(H^0(\Gamma_1))^3}) \\ &+ h^{4-\sigma}(\|B\|_{(H^{q+1}(\Gamma_2))^2} \times |U_n|_{(H^4(\Gamma_2))^3} + |U|_{(H^4(\Gamma_1))^3} + |U_n|_{(H^4(\Gamma_1))^3}) \\ &+ h^{q+1}|B|_{(H^{q+1}(\Gamma_2))^2} \times |M(U)|_{(H^0(\Gamma_2))^3}\}, \end{aligned} \tag{4.10}$$

where the notations are

$$|B|_{(H^k(\Gamma_2))^2} = \{|b_1|^2_{H^k(\Gamma_2)} + |b_2|^2_{H^k(\Gamma_2)}\}^{1/2}, \qquad \|B\|_{(H^k(\Gamma_2))^2} = \{\|b_1\|^2_{H^k(\Gamma_2)} + \|b_2\|^2_{H^k(\Gamma_2)}\}^{1/2}. \tag{4.11}$$

Corollary 4.3. *Let all the conditions in Theorem* 4.2 *and* $\sigma = 2$ *and* $q = 3$ *hold. When* $h \to 0$ *the solutions from the BP-FEMs* (3.12) *have the following asymptotes*:

$$|\,\|U - U_h^*\|\,| = \mathrm{O}(h^2), \qquad \|U - U_h^*\|_{(H^2(\Omega))^3} = \mathrm{O}(h^2), \tag{4.12}$$

$$\|\delta U_h^*\|_{[0,1]} = \mathrm{O}(h^4), \qquad \|\delta(U_h^*)_n\|_{[0,1]} = \mathrm{O}(h^4),$$

$$\|(y_h^*)_n - \bar{b}_1(x_h^*)_n\|_{H^0(\Gamma_2)} = \mathrm{O}(h^4), \qquad \|(z_h^*)_n - \bar{b}_2(x_h^*)_n\|_{H^0(\Gamma_2)} = \mathrm{O}(h^4), \tag{4.13}$$

$$\|(y_h^*)_n - b_1(x_h^*)_n\|_{H^0(\Gamma_2)} = \mathrm{O}(h^4), \qquad \|(z_h^*)_n - b_2(x_h^*)_n\|_{H^0(\Gamma_2)} = \mathrm{O}(h^4), \tag{4.14}$$

where

$$\|\delta U\|_{[0,1]} = \left\{\int_0^1 ((x(r,0) - x(r,1))^2 + (y(r,0) - y(r,1))^2 + (z(r,0) - z(r,1))^2)\,\mathrm{d}r\right\}^{1/2} \tag{4.15}$$

4.2. Superconvergence

Next consider superconvergence also for $\mu \in [0, \frac{1}{2})$ and choose the variant (3.16) of BP-FEM. We also use the notations

$$\overline{\|f\|}_{H^0(\Gamma_2)} = \left(\int_{\Gamma_2} (\Pi_p^5 f_I)^2\,\mathrm{d}\ell\right)^{1/2}, \quad \overline{\|f\|}_{H^0(\Gamma_0)} = \left(\int_{\Gamma_0} (f_I)^2\,\mathrm{d}\ell\right)^{1/2}. \tag{4.16}$$

Define a new norm involving discrete summation on $\delta\Omega$:

$$\overline{|\,\|U\|\,|} = (\|U\|^2_{(H^2(\Omega))^3} + \hat{D}(U,U))^{1/2}, \tag{4.17}$$

$$\begin{aligned} \hat{D}(U,U) = \frac{P_c}{h^{2\sigma}}\{&\overline{\|y_n - b_1 x_n\|}^2_{H^0(\Gamma_2)} + \overline{\|z_n - b_2 x_n\|}^2_{H^0(\Gamma_2)} \\ &+ \overline{\|U^+ - U^-\|}^2_{H^0(\Gamma_0)} + \overline{\|U_n^+ - U_n^-\|}^2_{H^0(\Gamma_0)}\}, \end{aligned}$$

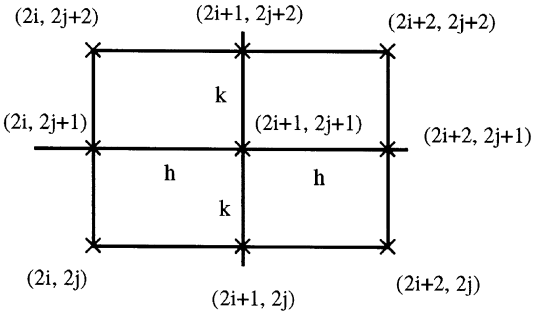

Fig. 4. $\square^{2\times 2}_{2i+1,2j+1}$ in the 2×2 fashion of partition.

where $\hat{D}(U,W)$ are given as (3.18). Note that the new norm definitions as in (4.17) are crucial to achieve the superconvergence for the solutions involving the boundary conditions. First from the integration rules in $\hat{D}(U,W)$ given by (3.20)–(3.25) we have the following lemma directly.

Lemma 4.4. *Let U, U_I and $\Pi_p^5 U_I$ be the true solutions, the piecewise cubic Hermite interpolants and the Hermite interpolants with order 5 on $\square^{2\times 2}_{2i+1,2j+1}$ respectively* (see Fig. 4), *then there exist the equalities*

$$\hat{D}(U,W)=0,\quad \hat{D}(U-U_I,W)=0,\quad \hat{D}(U-\Pi_p^5 U_I,W)=0,\quad \forall W\in V_h^0. \tag{4.18}$$

Lemma 4.5. *Let $f_n=\eta_n-b_1\xi_n$ and $b_1\in H^6(\Gamma_2)$, then there exist the bounds*

$$\|f_n\|_{H^0(\Gamma_2)}\leqslant C(h^\sigma+h^{3.5}\|b_1\|_{H^6(\Gamma_2)})|\!|\!|W|\!|\!|. \tag{4.19}$$

Proof. We have

$$\begin{aligned}\|f_n\|_{H^0(\Gamma_2)}-\overline{|\!|\!|f_n|\!|\!|}_{H^0(\Gamma_2)} &= \|f_n\|_{H^0(\Gamma_2)}-\|\hat{f}_n\|_{H^0(\Gamma_2)}\\ &\leqslant \|f_n-\hat{f}_n\|_{H^0(\Gamma_2)}=\|b_1\xi_n-\widehat{b_1\xi_n}\|_{H^0(\Gamma_2)}\\ &\leqslant Ch^6\|b_1\xi_n\|_{H^6(\Gamma_2)}\leqslant Ch^6\|b_1\|_{H^6(\Gamma_2)}\|\xi_n\|_{H^3(\Gamma_2)}\\ &\leqslant Ch^{3.5}\|b_1\|_{H^6(\Gamma_2)}|\!|\!|W|\!|\!|,\end{aligned} \tag{4.20}$$

where we have used the inequality for $W\in V_h^0$

$$\|\xi_n\|_{H^3(\Gamma_2)}\leqslant Ch^{-2.5}\|\xi_n\|_{H^{1/2}(\Gamma_2)}\leqslant Ch^{-2.5}\|\xi_n\|_{H^2(\Omega)}\leqslant Ch^{-2.5}|\!|\!|W|\!|\!|. \tag{4.21}$$

Since $\overline{|\!|\!|f_n|\!|\!|}_{H^0(\Gamma_2)}\leqslant Ch^\sigma\hat{D}(U,U)^{1/2}\leqslant Ch^\sigma|\!|\!|W|\!|\!|$, the desired results (4.19) are obtained. This completes the proof of Lemma 4.5. □

Lemma 4.6. *Let $M(U)\in(H^0(\Gamma))^3$, $P(U)\in(H^0(\Gamma_1))^3$, $F\in(H^4(\Omega))^3$, $B\in(H^6(\Gamma_2))^2$, and $\hat{F}$ in* (3.13) *be the piecewise cubic Hermite interpolants of F. For $\mu\in[0,\frac{1}{2})$ there exists a bounded*

constant C independent of h and σ such that

$$\overline{|\|U_I - \hat{U}_h^*\|\,|} \leqslant \varepsilon = C\left\{\frac{A(U-U_I,E)}{\overline{|\|E\|\,|}} + h^{\sigma}(|M(U)|_{(H^0(\Gamma))^3} + |P(U)|_{(H^0(\Gamma_1))^3}) \right.$$

$$\left. + h^{3.5}\|B\|_{(H^6(\Gamma_2))^2} \times |M(U)|_{(H^0(\Gamma_2))^3} + h^4|F|_{(H^4(\Omega))^3}\right\}, \tag{4.22}$$

where $U(\in H)$ and U_I are the true solutions and their piecewise cubic Hermite interpolants, respectively, and $\hat{U}_h^*(\in V_h)$ are the solutions from the BP-FEM given in (3.16).

Proof. Since the true solutions U satisfy natural boundary conditions (2.8) and (2.9), we can obtain the following equations by applying the Green theorem:

$$\begin{aligned} A(U,W) = &\iint_{\Omega} F\cdot W\,\mathrm{d}s + \int_{\Gamma_2}\{m(y)(\eta_n - b_1\xi_n) + m(z)(\zeta_n - b_2\xi_n)\}\,\mathrm{d}\ell \\ &+ \int_0^1 P(U(r,0))\cdot(W(r,0) - W(r,0))\,\mathrm{d}r \\ &+ \int_0^1 M(U(r,0))\cdot(W_n(r,0) - W_n(r,1))\,\mathrm{d}r = 0, \quad W\in V_h^0, \end{aligned} \tag{4.23}$$

where $m(x)$ and $m(y)$ are the components of the vector $M(U)$ defined in (2.10). Then we obtain from Lemma 4.4

$$\hat{A}_P(U,W) = A(U,W) + \hat{D}(U,W) = A(U,W), \quad W\in V_h^0. \tag{4.24}$$

Since solutions $\hat{U}_h^*$ satisfy (3.16), we have from (4.23)

$$\begin{aligned} |\hat{A}_P(U-\hat{U}_h^*,W)| = &\left|\int_{\Gamma_2}\{m(y)(\eta_n - b_1\xi_n) + m(z)(\zeta_n - b_2\xi_n)\}\,\mathrm{d}\ell\right| \\ &+ \left|\int_0^1 P(U(r,0))\cdot(W(r,0) - W(r,1))\,\mathrm{d}r\right| \\ &+ \left|\int_0^1 M(U(r,0))\cdot(W_n(r,0) - W_n(r,1))\,\mathrm{d}r\right| \\ &+ \left|\iint_{\Omega}(F-\hat{F})\cdot W\,\mathrm{d}\Omega\right| \\ = &\,\mathrm{I} + \mathrm{II} + \mathrm{III} + \mathrm{IV}. \end{aligned} \tag{4.25}$$

For the first term in the right-hand side of the above equation, we have from the Schwarz inequality, Lemma 4.5 and definition of $\overline{|\|W\|\,|}$ in (4.17)

$$\begin{aligned} \mathrm{I} &= \left|\int_{\Gamma_2}\{m(y)(\eta_n - b_1\xi_n) + m(z)(\zeta_n - b_2\xi_n)\}\,\mathrm{d}\ell\right| \\ &\leqslant C|M(U)|_{(H^0(\Gamma_2))^3} \times \left\{\int_{\Gamma_2}(|\eta_n - b_1\xi_n|^2 + |\zeta_n - b_2\xi_n|^2)\,\mathrm{d}\ell\right\}^{1/2} \end{aligned}$$

$$\leqslant C(h^{\sigma}+h^{3.5}\|B\|_{H^6(\Gamma_2))^2})|M(U)|_{H^0(\Gamma_2))^3}\times\overline{|\,\|W\|\,|}. \tag{4.26}$$

Next we estimate the rest terms in (4.25), we have again from (4.2)

$$\begin{aligned}
\mathrm{II} &= \left|\int_0^1 P(U(r,0))\cdot(W(r,0)-W(r,1))\,\mathrm{d}\ell\right| \\
&\leqslant |P(U)|_{(H^0(\overline{AB}))^3}\times\left(\int_0^1 \|W(r,0)-W(r,1)\|^2\,\mathrm{d}\ell\right)^{1/2} \\
&= |P(U)|_{(H^0(\overline{AB}))^3}\times\left(\widehat{\int_0^1} \|W(r,0)-W(r,1)\|^2\,\mathrm{d}\ell\right)^{1/2} \\
&\leqslant Ch^{\sigma}|P(U)|_{(H^0(\Gamma_0))^3}\times\hat{D}(W,W)^{1/2} \\
&\leqslant Ch^{\sigma}|P(U)|_{(H^0(\Gamma_0))^3}\times\overline{|\,\|W\|\,|}
\end{aligned} \tag{4.27}$$

and

$$\begin{aligned}
\mathrm{III} &= \left|\int_0^1 M(U(r,0))\cdot(W_n(r,0)-W_n(r,1))\,\mathrm{d}r\right| \\
&\leqslant Ch^{\sigma}|M(U)|_{(H^0(\Gamma_0))^3}\times\overline{|\,\|W\|\,|}.
\end{aligned} \tag{4.28}$$

Since $\bar{F}$ is piecewise cubic Hermite interpolant of F, we have

$$\begin{aligned}
\mathrm{IV} &= \left|\iint_{\Omega}(F-\hat{F})\cdot W\,\mathrm{d}\Omega\right| \leqslant Ch^4|F|_{(H^4(\Omega))^3}\times\|W\|_{(H^0(\Omega))^3} \\
&\leqslant Ch^4|F|_{(H^4(\Omega))^3}\times\overline{|\,\|W\|\,|}.
\end{aligned} \tag{4.29}$$

Therefore, combining (4.25)–(4.29) leads to

$$|\hat{A}_P(U-\hat{U}_h^*,W)|\leqslant \mathrm{I}+\mathrm{II}+\mathrm{III}+\mathrm{IV}\leqslant CQ\overline{|\,\|W\|\,|}, \tag{4.30}$$

where

$$Q=h^{\sigma}(|M(U)|_{(H^0(\Gamma))^3}+|P(U)|_{(H^0(\Gamma_0))^3})+h^{3.5}|B|_{(H^6(\Gamma_2))^2}\times|M(U)|_{(H^0(\Gamma_2))^3}+h^4|F|_{(H^4(\Omega))^3}.$$

Moreover, letting $E=U_I-\hat{U}_h^*$ then $E\in V_h^0$. Hence $\hat{D}(U-U_I,E)=0$ from Lemma 4.4. We obtain also from Lemma 4.1 and (4.30) that

$$\begin{aligned}
C_0\overline{|\,\|E\|\,|}^2 &\leqslant \hat{A}_P(E,E)\leqslant 2(|\hat{A}_P(U-U_I,E)|+|\hat{A}_P(U_I-\hat{U}_h^*,E)|) \\
&\leqslant C(|\hat{A}(U-U_I,E)|+|\hat{D}(U-U_I,E)+Q\times\overline{|\,\|E\|\,|}) \\
&\leqslant C_1\left(\frac{A(U-U_I,E)}{\overline{|\,\|E\|\,|}}+Q\right)\times\overline{|\,\|E\|\,|}.
\end{aligned} \tag{4.31}$$

The desired results (4.22) are obtained by dividing two sides of (4.31) by $\overline{|\,\|E\|\,|}$. This completes the proof of Lemma 4.6. □

Now we derive the important bounds for $A(U-U_I,E)$ needed in Lemma 4.6, where

$$A(U,W)=\int\!\!\int_{\Omega}\{U_{rr}\cdot W_{rr}+U_{tt}\cdot W_{rr}+2(1-\mu)U_{rt}\cdot W_{rt}+\mu(U_{rr}\cdot W_{tt}+U_{tt}\cdot W_{rr})\}\,\mathrm{d}r\,\mathrm{d}t, \tag{4.32}$$

whose bounds are derived by the following three lemmas.

Lemma 4.7. *For $W\in V_h^0$ there exist the bounds for quasiuniform $\square_{ij}$*

$$\left|\int\!\!\int_{\Omega}(U-U_I)_{rr}\cdot W_{rr}\,\mathrm{d}r\,\mathrm{d}t\right|\leqslant Ch^4\|U\|_{(H^6(\Omega))^3}\overline{|\,\|W\|\,|}\ (\text{or } Ch^3\|U\|_{(H^5(\Omega))^3}\overline{|\,\|W\|\,|}), \tag{4.33}$$

for quasiuniform $\square_{ij}$

$$\left|\int\!\!\int_{\Omega}(U-U_I)_{rt}\cdot W_{rt}\,\mathrm{d}r\,\mathrm{d}t\right|\leqslant Ch^3\|U\|_{(H^5(\Omega))^3}\overline{|\,\|W\|\,|}, \tag{4.34}$$

but for uniform $\square_{ij}$

$$\left|\int\!\!\int_{\Omega}(U-U_I)_{rt}\cdot W_{rt}\,\mathrm{d}r\,\mathrm{d}t\right|\leqslant C\left(h^4\|U\|_{(H^6(\Omega))^3}+h^{3.5}\left\|\frac{\partial^4U}{\partial n^4}\right\|_{(H^1(\Gamma_2))^3}+h^{3+\sigma}\left\|\frac{\partial^4U}{\partial n^4}\right\|_{(H^1(\Gamma_0))^3}\overline{|\,\|W\|\,|}\right). \tag{4.35}$$

Proof. Eqs. (4.33) and (4.34) follow directly from Li [26] (also see [27–29]. For uniform $\square_{ij}$, we also have the bounds from Lemma 4.1 of paper [26]:

$$\left|\int\!\!\int_{\Omega}(U-U_I)_{rt}\cdot W_{rt}\,\mathrm{d}r\,\mathrm{d}t\right|\leqslant Ch^4\left(\|U\|_{(H^6(\Omega))^3}\overline{|\,\|W\|\,|}+\left\|\frac{\partial^4U}{\partial n^4}\right\|_{(H^1(\Gamma_2))^3}\|W_n\|_{(H^1(\Gamma_2))^3}+\left\|\frac{\partial^4U}{\partial n^4}\right\|_{(H^1(\Gamma_0))^3}\|W_n^+-W_n^-\|_{(H^1(\Gamma_0))^3}\right). \tag{4.36}$$

Then we have

$$\|W_n\|_{(H^1(\Gamma_2))^3}\leqslant Ch^{-1/2}\|W_n\|_{(H^{1/2}(\Gamma_2))^3}\leqslant Ch^{-1/2}\|W\|_{(H^2(\Omega))^3}\leqslant Ch^{-1/2}\overline{|\,\|W\|\,|}, \tag{4.37}$$

$$\begin{aligned}\|W_n^+-W_n^-\|_{(H^1(\Gamma_0))^3}&\leqslant Ch^{-1}\|W_n^+-W_n^-\|_{(H^0(\Gamma_0))^3}\\&=Ch^{-1}\|\overline{W_n^+-W_n^-}\|_{(H^0(\Gamma_0))^3}\leqslant Ch^{\sigma-1}\overline{|\,\|W\|\,|}.\end{aligned} \tag{4.38}$$

The desired results (4.35) are obtained from (4.36)–(4.38). This completes the proof of Lemma 4.7. □

Lemma 4.8. *Let $\mu\in[0,\frac{1}{2})$ $U\in V_h$ and $W\in V_h^0$. Then there exist the bounds for quasiuniform $\square_{ij}$*

$$\left|\int\!\!\int_{\Omega}(U-U_I)_{rr}\cdot W_{tt}\,\mathrm{d}r\,\mathrm{d}t\right|\leqslant\left|\int\!\!\int_{\Omega}(U-U_I)_{rt}\cdot W_{rt}\,\mathrm{d}r\,\mathrm{d}t\right|+Ch^{2+\sigma}|U|_{(H^4(\Gamma_0))^3}\overline{|\,\|W\|\,|} \tag{4.39}$$

and

$$\left|\int\int_{\Omega}(U-U_I)_{tt}\cdot W_{rr}\,\mathrm{d}r\,\mathrm{d}t\right| \leqslant \left|\int\int_{\Omega}(U-U_I)_{rt}\cdot W_{rt}\,\mathrm{d}r\,\mathrm{d}t\right| + Ch^{2+\sigma}|U_n|_{(H^4(\Gamma_0))^3}\overline{|\,\|W\|\,|}. \quad (4.40)$$

Proof. In fact, the functions $(U-U_I)_r$, W (and W_{tt}) are continuous along the edges parallel to axis t, and $W_{tt}=0$ on Γ_2 for $W\in V_h^0$. Hence we obtain from integration by parts

$$\int\int_{\Omega}(U-U_I)_{rr}\cdot W_{tt}\,\mathrm{d}r\,\mathrm{d}t = -\int\int_{\Omega}(U-U_I)_r\cdot W_{rtt}\,\mathrm{d}r\,\mathrm{d}t, \quad W\in V_h^0. \quad (4.41)$$

Similary, since the functions $(U-U_I)_r$ and W_{rt} are continuous along the edges parallel to axis r for $W\in V_h^0$ and the periodical solutions U at $t=0,1$

$$\int\int_{\Omega}(U-U_I)_r\cdot W_{rtt}\,\mathrm{d}r\,\mathrm{d}t = -\int\int_{\Omega}(U-U_I)_{rt}\cdot W_{rt}\,\mathrm{d}r\,\mathrm{d}t + \int_{\Gamma_0}(U-U_I)_r\cdot(W_{rt}^+ - W_{rt}^-)\,\mathrm{d}r, \quad W\in V_h^0. \quad (4.42)$$

Combining (4.41) and (4.42) yields

$$\int\int_{\Omega}(U-U_I)_{rr}\cdot W_{tt}\,\mathrm{d}r\,\mathrm{d}t = \int\int_{\Omega}(U-U_I)_{rt}\cdot W_{rt}\,\mathrm{d}r\,\mathrm{d}t - \int_{\Gamma_0}(U-U_I)_r\cdot(W_{rt}^+ - W_{rt}^-)\,\mathrm{d}r, \quad W\in V_h^0. \quad (4.43)$$

Also we have

$$\left|\int_{\Gamma_0}(U-U_I)_r\cdot(W_{rt}^+ - W_{rt}^-)\,\mathrm{d}r\right| \leqslant |U-U_I|_{(H^1(\Gamma_0))^3}\|W_n^+ - W_n^-\|_{(H^1(\Gamma_0))^3} \quad (4.44)$$

and

$$|U-U_I|_{(H^1(\Gamma_0))^3} \leqslant Ch^3|U|_{(H^4(\Gamma_0))^3}. \quad (4.45)$$

The first bounds (4.39) follow from (4.43)–(4.45) and (4.38). Below we prove (4.40).

Similarly, by noting $U\in V_h$ and $W\in V_h^0$ we obtain from integration by parts

$$\int\int_{\Omega}(U-U_I)_{tt}\cdot W_{rr}\,\mathrm{d}r\,\mathrm{d}t = \int\int_{\Omega}(U-U_I)_{rt}\cdot W_{rt}\,\mathrm{d}r\,\mathrm{d}t + \int_{\Gamma_0}(U-U_I)_t\cdot(W_{rr}^+ - W_{rr}^-)\,\mathrm{d}r - \int_{\Gamma_2}(U-U_I)_t\cdot W_{rt}\,\mathrm{d}t. \quad (4.46)$$

Moreover, we have from (4.38)

$$\begin{aligned}\left|\int_{\Gamma_0}(U-U_I)_t\cdot(W_{rr}^+ - W_{rr}^-)\,\mathrm{d}r\right| &\leqslant |(U-U_I)_n|_{(H^0(\Gamma_0))^3}\|W_n^+ - W_n^-\|_{(H^2(\Gamma_0))^3}\\ &\leqslant Ch^4|U_n|_{(H^4(\Gamma_0))^3}\times h^{-2}\overline{\|W_n^+ - W_n^-\|}_{(H^0(\Gamma_0))^3}\\ &\leqslant Ch^{2+\sigma}|U_n|_{(H^4(\Gamma_0))^3}\overline{|\,\|W\|\,|}. \end{aligned} \quad (4.47)$$

Note that the assumption $U \in V_h$ indicates $g = U|_{\Gamma_2} = U_I$. Hence we obtain also from integration by parts

$$\int_{\Gamma_2} (U - U_I)_t \cdot W_{rt}\, \mathrm{d}t = -\int_{\Gamma_2} (U - U_I) \cdot W_{rtt}\, \mathrm{d}t = -\int_{\Gamma_2} (g - U_I) \cdot W_{rtt}\, \mathrm{d}t = 0. \tag{4.48}$$

Combining (4.46)–(4.48) leads to the second desired results (4.40). This completes the proof of Lemma 4.8. □

By noting (4.32) and applying Lemmas 4.7 and 4.8 we obtain the following lemma.

Lemma 4.9. *Let $\mu \in [0, \frac{1}{2})$, $U \in V_h$ and $W \in V_h^0$. Then there exist the bounds for quasiuniform $\square_{ij}$*

$$A(U - U_I, W) \leqslant C\{h^3 \|U\|_{(H^5(\Omega))^3} + h^{2+\sigma}(|U_n|_{(H^4(\Gamma_0))^3} + |U|_{(H^4(\Gamma_0))^3})\}\overline{|\,\|W\|\,|}, \tag{4.49}$$

and for uniform $\square_{ij}$

$$A(U - U_I, W) \leqslant C\left\{h^4 \|U\|_{(H^6(\Omega))^3} + h^{3.5}\left\|\frac{\partial^4 U}{\partial n^4}\right\|_{(H^1(\Gamma_2))^3} + h^{3+\sigma}\left\|\frac{\partial^4 U}{\partial n^4}\right\|_{(H^1(\Gamma_0))^3} + h^{2+\sigma}(|U_n|_{(H^4(\Gamma_0))^3} + |U|_{(H^4(\Gamma_0))^3})\right\}\overline{|\,\|W\|\,|}. \tag{4.50}$$

Also construct the a posteriori interpolants $\Pi_p^5 \hat{U}_h^*$ of order 5 on $\square_{ij}^{2\times 2}$. We have the following theorem.

Theorem 4.10. *Let $\mu \in [0, \frac{1}{2})$ and all conditions in Lemma 4.6 hold. Then there exist the bounds*

$$\overline{|\,\|U - \Pi_p^5 \hat{U}_h^*\|\,|} \leqslant \varepsilon = C\{R + h^4 |F|_{(H^4(\Omega))^3} + h^{\sigma}(|M(U)|_{(H^0(\Gamma))^3} + |P(U)|_{(H^0(\Gamma_1))^3}) + h^{3.5}\|B\|_{(H^6(\Gamma_2))^2} \times |M(U)|_{(H^0(\Gamma_2))^3}\}, \tag{4.51}$$

where

$$R = h^3 \|U\|_{(H^5(\Omega))^3} + h^{2+\sigma}(|U_n|_{(H^4(\Gamma_0))^3} + |U|_{(H^4(\Gamma_0))^3}) \tag{4.52}$$

for quasiuniform $\square_{ij}$, and

$$R = h^4 \|U\|_{(H^6(\Omega))^3} + h^{3.5}\left\|\frac{\partial^4 U}{\partial n^4}\right\|_{(H^1(\Gamma_2))^3} + h^{3+\sigma}\left\|\frac{\partial^4 U}{\partial n^4}\right\|_{(H^1(\Gamma_0))^3} + h^{2+\sigma}(|U_n|_{(H^4(\Gamma_0))^3} + |U|_{(H^4(\Gamma_0))^3}) \tag{4.53}$$

for uniform $\square_{ij}$.

Proof. Let $W = U - \Pi_p^5 U_I$. We have $\hat{D}(W, W) = 0$ from Lemma 4.2. Hence, we have from Lemma 4.4 and [26]

$$\begin{aligned}\overline{|\,\|U - \Pi_p^5 \hat{U}_h^*\|\,|} &\leqslant \overline{|\,\|U - \Pi_p^5 U_I\|\,|} + \overline{|\,\|\Pi_p^5(U_I - \hat{U}_h^*)\|\,|} \\ &\leqslant \|U - \Pi_p^5 U_h^*\|_{(H^2(\Omega))^3} + \hat{D}(W, W)^{1/2} + C\overline{|\,\|U_I - \hat{U}_h^*\|\,|} \\ &\leqslant \|U - \Pi_p^5 U_h^*\|_{(H^2(\Omega))^3} + C\overline{|\,\|U_I - \hat{U}_h^*\|\,|} \leqslant C(h^v \|U\|_{(H^{v+2}(\Omega))^3} + \varepsilon), \quad v = 3, 4,\end{aligned} \tag{4.54}$$

where ε is given in Lemma 4.6. The desired results are obtained from Lemmas 4.6 and 4.9. □

Corollary 4.11. *Let* $U \in (H^{v+2}(\Omega))^3$ $(v=3,4)$, $U \in (H^4(\Gamma_0))^3$, $U_n \in (H^4(\Gamma_0))^3$, $\partial^4 U/\partial n^4 \in (H^1(\Gamma_0))^3$, $\partial^4 U/\partial n^4 \in (H^1(\Gamma_2))^3$, *and all the conditions in Lemma* 4.6 *hold. Then when* $\sigma = 3 \wedge v = 3$ *and* $\sigma=3.5\wedge v=4$ *for quasiuniform and uniform* $\square_{ij}$, *respectively*, *the solutions from the BP-FEM*, (3.16), *have the following superconvergence as* $h \to 0$:

$$\overline{|\,\|U - \Pi_p^5 \hat{U}_h^*\|\,|} = \mathrm{O}(h^\sigma), \quad \|U_I - \hat{U}_h^*\|_{(H^2(\Omega))^3} = \mathrm{O}(h^\sigma), \tag{4.55}$$

$$\|\delta \hat{U}_h^*\|_{[0,1]} = \mathrm{O}(h^{2\sigma}), \quad \|\delta(U_h^*)_n\|_{[0,1]} = \mathrm{O}(h^{2\sigma}), \tag{4.56}$$

$$\overline{\|\delta \Pi_p^5 \hat{U}_h^*\|}_{[0,1]} = \mathrm{O}(h^{2\sigma}), \quad \overline{\|\delta \Pi_p^5 (\hat{U}_h^*)_n\|}_{[0,1]} = \mathrm{O}(h^{2\sigma}), \tag{4.57}$$

$$\overline{\|\Pi_p^5(\hat{y}_h^*)_n - b_1 \Pi_p^5(\hat{x}_h^*)_n\|}_{H^0(\Gamma_2)} = \mathrm{O}(h^{2\sigma}), \tag{4.58}$$

$$\overline{\|\Pi_p^5(\hat{z}_h^*)_n - b_2 \Pi_p^5(\hat{x}_h^*)_n\|}_{H^0(\Gamma_2)} = \mathrm{O}(h^{2\sigma}). \tag{4.59}$$

Remark 1. Contrasted to $\mathrm{O}(h^8)$ of the boundary constraints for uniform $\square_{ij}$ in [26], only $\mathrm{O}(h^7)$ of superconvergence can be attained. The reason for such one order loss in superconvergence is not the extension from $\mu = 0$ to $\mu \in [0, \frac{1}{2})$, but the complexity of the boundary constraints in the penalty integrals (3.15) on Γ_2. In fact, we may easily extend all the high superconvergence in [26] from $\mu = 0$ to $\mu \in [0, \frac{1}{2})$, by the help of new estimates (4.43) and (4.46) in Lemma 4.8 in this paper. Besides, for the purposes of blending only, we may not need the a posteriori interpolant $\Pi_p^4 \hat{U}_h^*$ over Ω because our attention is focussed on the boundary matching. Hence only the a posterior interpolant on Γ_2 as in (3.25) will lead to the superconvergence (4.56), (4.58) and (4.59).

4.3. Stability

Finally, we provide stability analysis for the BP-FEM (3.12) which is written as a system of linear algebraic equations

$$\mathbf{T}\boldsymbol{w} = \boldsymbol{k}, \tag{4.60}$$

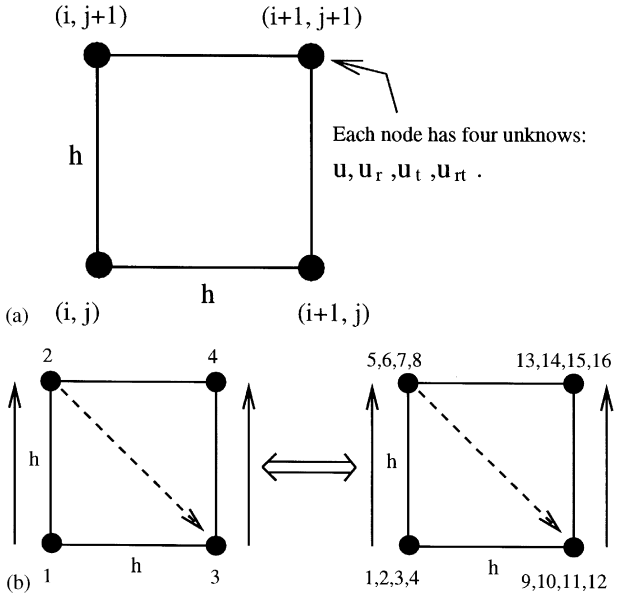

Fig. 5. (a) Element $\square_{ij}$ with the boundary length h. (b) The order of 16 unknowns on $\square_{ij}$: $v_1, (v_r)_1, (v_t)_1, (v_{rt})_1, v_2, (v_r)_2, (v_t)_2, (v_{rt})_2, v_3, (v_r)_3, (v_t)_3, (v_{rt})_3$ and $v_4, (v_r)_4, (v_t)_4, (v_{rt})_4$.

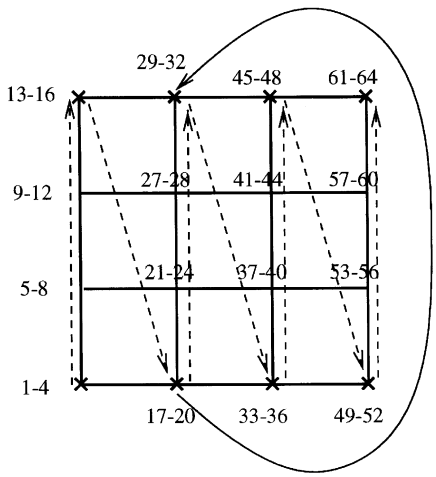

Fig. 6. The order of all unknowns u_1–u_{64} in a 3×3 partition of Ω.

where $\boldsymbol{w} = (\ldots, x^*_{ij}, (x_r)^*_{ij}, (x_t)^*_{ij}, (x^*_{rt})_{ij}, y^*_{ij}, (y_r)^*_{ij}, (y_t)^*_{ij}, (y^*_{rt})_{ij}, z^*_{ij}, (z_r)^*_{ij}, (z_t)^*_{ij}, (z^*_{rt})_{ij}, \ldots)^{\mathrm{T}}$, $\boldsymbol{k}$ is a known vector, and $\mathbf{T}$ is symmetric and positive-definite matrix. The order of variables shown as in Figs. 5 and 6 and may reduce the matrix bandwidth. The numerical stability is measured by the condition number: $cond.(\mathbf{T}) = \lambda_{\max}(\mathbf{T})/\lambda_{\min}(\mathbf{T})$ of matrix $\mathbf{T}$, where $\lambda_{\max}(\mathbf{T})$ and $\lambda_{\min}(\mathbf{T})$ are the maximal and minimal eigenvalues of $\mathbf{T}$. We do not follow in detail the proof in [26], but find out the relation of the analysis between in [26] and in this paper.

Let us first consider one biharmonic equation and the clamped and periodical conditions on the unit square Ω as in [26]

$$\Delta^2 u = \left(\frac{\partial^2}{\partial r^2} + \frac{\partial^2}{\partial t^2}\right)^2 u = f, \quad (r,t) \in \Omega, \tag{4.61}$$

$$u = g, \quad \frac{\partial u}{\partial n} = g_1 \quad \text{on } \Gamma_2, \tag{4.62}$$

$$u(r,0) = u(r,1), \quad u_t(r,0) = u_t(r,1), \quad 0 \leqslant r \leqslant 1, \tag{4.63}$$

where n is the outward normal of $\partial\Omega$, and Ω is a unit square: $\Omega = \{(r,t),\ 0 \leqslant r \leqslant 1,\ 0 \leqslant t \leqslant 1\}$, shown in Fig. 2. In fact, Eqs. (4.61)–(4.63) are a special case of the 3D problems of blending surfaces given in this paper. The corresponding BP-FEM is expressed by: To seek u_h such that

$$b(u_h, v) = F(v), \tag{4.64}$$

where u_h and v are the functions (3.4) satisfying $(u_h)|_{\Gamma_0} = g$ and $v|_{\Gamma_0} = 0$, respectively. The notations are

$$b(u,v) = \iint_\Omega \Lambda_\mu(u,v)\,\mathrm{d}s + D(u,v), \tag{4.65}$$

$$F(v) = f(v) + \frac{P_c}{h^{2\sigma}} \int_{\Gamma_2} g_1 v_n \,\mathrm{d}\ell, \tag{4.66}$$

$$D(u,v) = \frac{P_c}{h^{2\sigma}} \left\{ \int_{\Gamma_2} u_n v_n \,\mathrm{d}\ell + \int_0^1 (u^+ - u^-)(v^+ - v^-)\,\mathrm{d}r + \int_0^1 (u_t^+ - u_t^-)(v_t^+ - v_t^-)\,\mathrm{d}r \right\}, \tag{4.67}$$

where $u^+ = u(r,1)$, $u^- = u(r,0)$, $\sigma(>0)$ is the penalty power, $P_c(>0)$ is a bounded constant independent of h, u and v, and $h = \max_{ij}(\delta r_i, \delta t_j)$. In (4.65), the integrands are

$$\Lambda_\mu(u,v) = u_{rr}v_{rr} + u_{tt}v_{tt} + 2(1-\mu)u_{rt}v_{rt} + \mu(u_{rr}v_{tt} + u_{tt}v_{rr}). \tag{4.68}$$

In [26], we have derived the estimates for the condition number of the associated matrix $\mathbf{A}$ under $\mu = 0$ in (4.64); all the arguments in [26] can be extended, word for word, to the condition number under $\mu \in [0, \frac{1}{2})$. We write the results without proof.

Lemma 4.12. *For $\mu \in [0, \frac{1}{2})$, there exist the bounds*

$$b(v,v) \leqslant C(h^{-2} + h^{1-2\sigma})(\boldsymbol{v}^*)^{\mathrm{T}}\boldsymbol{v}^*, \quad b(v,v) \geqslant C_0\|v\|_{H^2(\Omega)} \geqslant C_0 h^2 (\boldsymbol{v}^*)^{\mathrm{T}}\boldsymbol{v}^* \tag{4.69}$$

where $b(v,v) = (\boldsymbol{v}^*)^{\mathrm{T}}\mathbf{A}\boldsymbol{v}^*$, C and $C_0 > 0$ are two bounded constants independent of h and σ, and $\boldsymbol{x}^*$ is the vector consisting of x^*_{ij}, $(x^*_r)_{ij}$, $(x^*_t)_{ij}$ and $(x^*_{rt})_{ij}$.

Theorem 4.13. *Let $B \in (H^1(\Gamma_2))^2$ and $\mu \in [0, \frac{1}{2})$ hold. When $\square_{ij}$ are quasiuniform, then under the variable transformations* (3.5), *the condition number of matrix* $\mathbf{T}$ *resulting from the BP-FEM* (3.12) *has the following bounds*:

$$\text{contd.}(\mathbf{T}) \leqslant \mathbf{C}(h^{-4} + h^{-1-2\sigma}). \tag{4.70}$$

Proof. Consider

$$\bar{D}(U,U)=\frac{P_c}{h^{2\sigma}}\left\{\int_{\Gamma_2}(y_n-\bar{b}_1x_n)^2\,\mathrm{d}\ell+\int_{\Gamma_2}(z_n-\bar{b}_2x_n)^2\,\mathrm{d}\ell\right.$$
$$\left.+\int_0^1\|U(r,0)-U(r,1)\|^2\,\mathrm{d}r+\int_0^1\|U_n(r,0)-U_n(r,1)\|^2\,\mathrm{d}r\right\} \tag{4.71}$$

When $b_i\in H^1(\Gamma_2)$, $i=1,2$, the interpolants of b_i have the bounds,

$$\|\bar{b}_i\|_{0,\Gamma_2}\leqslant\|b_i\|_{0,\Gamma_2}+\|b_i-\bar{b}_i\|_{0,\Gamma_2}$$
$$\leqslant\|b_i\|_{0,\Gamma_2}+Ch|b_i|_{1,\Gamma_2}\leqslant C\|b_i\|_{1,\Gamma_2}\leqslant C \tag{4.72}$$

then

$$\int_{\Gamma_2}(y_n-\bar{b}_1x_n)^2\,\mathrm{d}\ell=\|y_n-\bar{b}_1x_n\|^2_{0,\Gamma_2}\leqslant 2\|y_n\|^2_{0,\Gamma_2}+2\|\bar{b}_1\|_{0,\Gamma_2}\|x_n\|^2_{0,\Gamma_2}$$
$$\leqslant C(\|y_n\|^2_{0,\Gamma_2}+\|x_n\|^2_{0,\Gamma_2})=C\int_{\Gamma_2}(y_n^2+x_n^2)\,\mathrm{d}\ell \tag{4.73}$$

Similarly,

$$\int_{\Gamma_2}(z_n-\bar{b}_2x_n)^2\,\mathrm{d}\ell=C\int_{\Gamma_2}(z_n^2+x_n^2)\,\mathrm{d}\ell \tag{4.74}$$

Hence we have

$$A_p(U,U)\leqslant C(b(x,x)+b(y,y)+b(z,z)), \tag{4.75}$$

where

$$b(v,v)=\iint_\Omega\Lambda_\mu(v,v)\,\mathrm{d}s+D(v,v). \tag{4.76}$$

Since $A_p(U,U)=\boldsymbol{w}^{\mathrm{T}}\mathbf{T}\boldsymbol{w}$ we have

$$\lambda_{\max}(\mathbf{T})=\max_{\boldsymbol{w}\neq 0}\frac{(\boldsymbol{w})^{\mathrm{T}}\mathbf{T}\boldsymbol{w}}{(\boldsymbol{w})^{\mathrm{T}}\boldsymbol{w}}=\max_{\boldsymbol{w}\neq 0}\frac{A_p(U,U)}{(\boldsymbol{w})^{\mathrm{T}}\boldsymbol{w}},$$

$$\lambda_{\min}(\mathbf{T})=\min_{\boldsymbol{w}\neq 0}\frac{(\boldsymbol{w})^{\mathrm{T}}\mathbf{T}\boldsymbol{w}}{(\boldsymbol{w})^{\mathrm{T}}\boldsymbol{w}}=\min_{\boldsymbol{w}\neq 0}\frac{A_p(U,U)}{(\boldsymbol{w})^{\mathrm{T}}\boldsymbol{w}},$$

to lead to

$$cond.(\mathbf{T})=\frac{\max_{\boldsymbol{w}\neq 0}(A_p(U,U)/(\boldsymbol{w})^{\mathrm{T}}\boldsymbol{w})}{\min_{\boldsymbol{w}\neq 0}(A_p(U,U)/(\boldsymbol{w})^{\mathrm{T}}\boldsymbol{w})}. \tag{4.77}$$

Denote the vector $w^{\mathrm{T}}=((x^*)^{\mathrm{T}},(y^*)^{\mathrm{T}},(z^*)^{\mathrm{T}})$ by permutation, where $(\boldsymbol{x}^*)^{\mathrm{T}}=(\ldots,(x^*)_{ij},(x^*_r)_{ij},(x^*_t)_{ij},(x^*_{rt})_{ij})$. Since $A_p(v,v)$ is invariant under any variable permutation, we obtain from (4.75) and Lemma 4.12 that

$$A_p(U,U)\leqslant C(h^{-2}+h^{1-2\sigma})((\boldsymbol{x}^*)^{\mathrm{T}}\boldsymbol{x}^*+(\boldsymbol{y}^*)^{\mathrm{T}}\boldsymbol{y}^*+(\boldsymbol{z}^*)^{\mathrm{T}}\boldsymbol{z}^*)$$
$$=C(h^{-2}+h^{1-2\sigma})(\boldsymbol{w})^{\mathrm{T}}\boldsymbol{w}. \tag{4.78}$$

Next it follows from (4.6) and Lemma 4.12 that

$$A_p(U,U) \geqslant C_0|\,\|U\|\,|^2 \geqslant C_0\|x\|^2_{H^2(\Omega)} + \|y\|^2_{H^2(\Omega)} + \|z\|^2_{H^2(\Omega)})$$
$$\geqslant C_0h^2((\boldsymbol{x}^*)^{\mathrm{T}}\boldsymbol{x}^* + (\boldsymbol{y}^*)^{\mathrm{T}}\boldsymbol{y}^* + (\boldsymbol{z}^*)^{\mathrm{T}}\boldsymbol{z}^*) = Ch^2(\boldsymbol{w})^{\mathrm{T}}\boldsymbol{w}. \tag{4.79}$$

Since C and $C_0(>0)$ are two bounded constants independent of h and σ, the desired results (4.70) follow from (4.77), (4.78) and (4.79). This completes the proof of Theorem 4.13. □

5. Examples for generating real blending surfaces

Since the verification on the theoretical analysis is given in [26], in this section the numerical experiments are designed to generate real samples of 3D blending surfaces; three different models are given (see [8]). The corresponding real blending surfaces $U(r,t) = (x,(r,t), y(r,t), z(r,t))^{\mathrm{T}}$ will be described by resembling flexibly elastic plates and obtained approximately by the BP-FEM in (3.12).

First, consider two separated and equal spheres with the same radius (=13) in Fig. 7(a). Both spheres are cut by vertical planes, and the circular gashes with the radius equal to 5 are obtained. We will generate a blending surface to connect the gashes, ∂V_1 and ∂V_2, of the left and the right spheres, V_1 and V_2. We provide below the boundary conditions of ∂V_1 and ∂V_2 in Fig. 7(a).

Example 5.1.

$$\Delta^2 U = F, \quad \text{in } \Omega,$$

$$\partial V_1 = (5\cos(t), 5\sin(t), r)^{\mathrm{T}}, \qquad (\partial V_1)_n = \left(\frac{-12\cos(t)}{5}, \frac{-12\sin(t)}{5}, 1\right)^{\mathrm{T}},$$

$$\partial V_2 = (5\cos(t), 5\sin(t), r)^{\mathrm{T}}, \qquad (\partial V_2)_n = \left(\frac{-12\cos(t)}{5}, \frac{-12\sin(t)}{5}, 1\right)^{\mathrm{T}},$$

where U and F are defined in (2.1) and (2.7); $t \in [0, 2\pi]$ and $r \in [12, 32]$.

Hence, from Sections 2 and 3, we use the BP-FEM (3.12) as $\mu = 0$ to evaluate the numerical solutions to the system of three biharmonic equations. Let the square solution area

$$\Omega = \{(r,t)\,|\,r \in [12,32], \quad t \in [0, 2\pi]\}$$

be divided into 8×4 uniform rectangular elements, i.e., choose $m = 8$ and $n = 4$ in Eqs. (3.1)–(3.7). Also, let $\bar{b}_i$ be the piecewise cubic Hermite interpolants of b_i, and choose $P_c = 20$ and $\sigma = 2$ in (3.15), which lead to the optimal convergence rates. We first consider the blending surface in *a natural state*, i.e., no external loading force on elastic plate: $F = (0,0,0)^{\mathrm{T}}$. Then after computing, the real blending surface of Example 5.1 is obtained and drawn by computer graphics in Fig. 7(b).

Note the *narrow channel* is formed by a closed blending surface between two spheres in Fig. 7(b); however we may expand the channel by adding the external (i.e., internal) loading forces F (see Fig. 8). As we describe the elastic plate as a blending surface, the expanding force in Fig. 8(a) will be restated as these external forces that act on the plate (see Fig. 8(b)). In fact, the forces in Fig. 7(c)–(e), consist of two nonzero components, which have the same magnitudes but

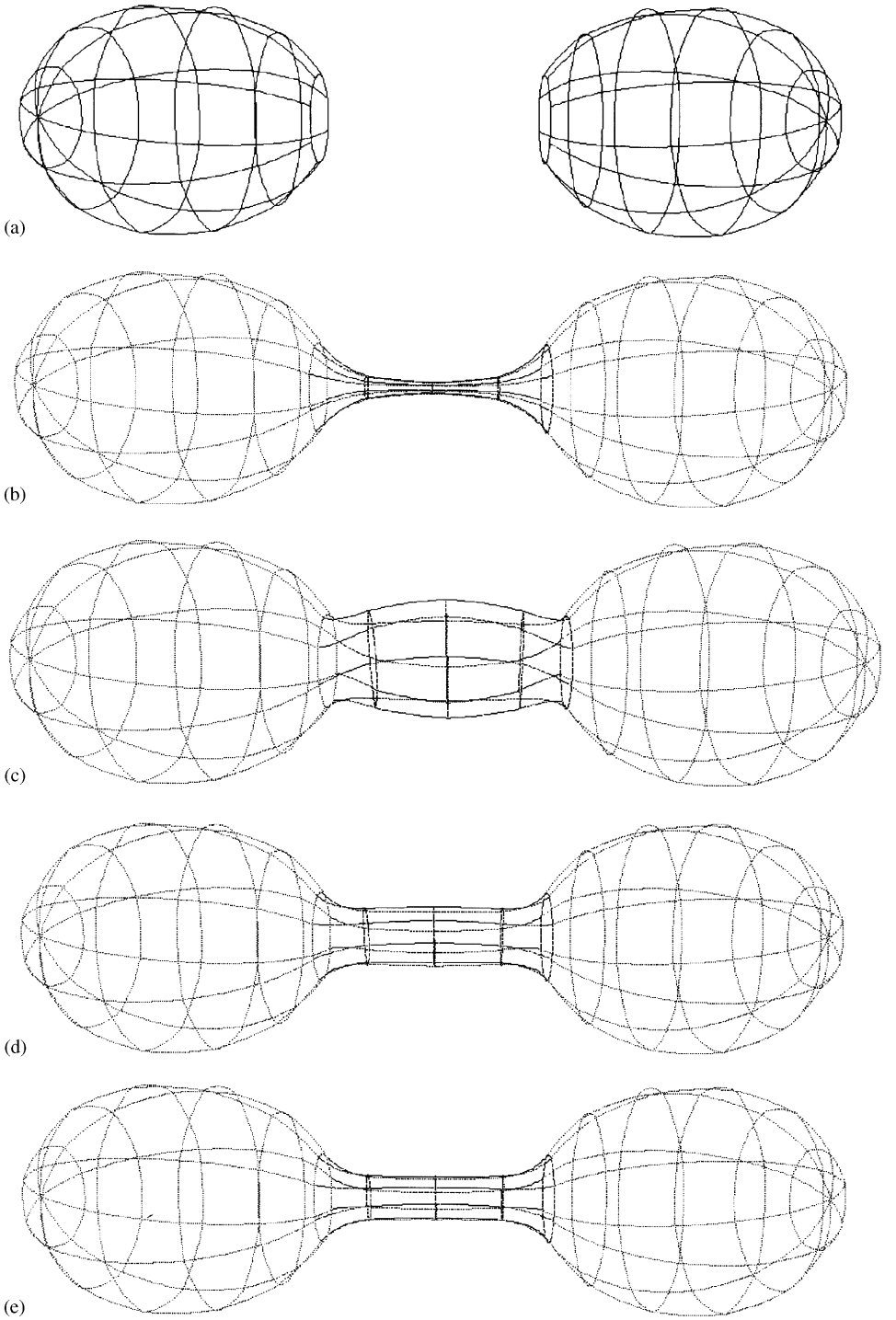

Fig. 7. (a) Two separated spheres with equal radii. (b) The blending surface by $F=(0,0,0)^{\mathrm{T}}$. (c) The blending surface by $F=(\mathrm{sign}(\sin(t)),\mathrm{sign}(\sin(t)),0)^{\mathrm{T}}$. (d) The blending surface by $F=(t\,\mathrm{sign}(\sin(t)),t\,\mathrm{sign}(\sin(t)),0)^{\mathrm{T}}$. (e) The blending surface by $F=(t^2\,\mathrm{sign}(\sin(t)),t^2\,\mathrm{sign}(\sin(t)),0)^{\mathrm{T}}$.

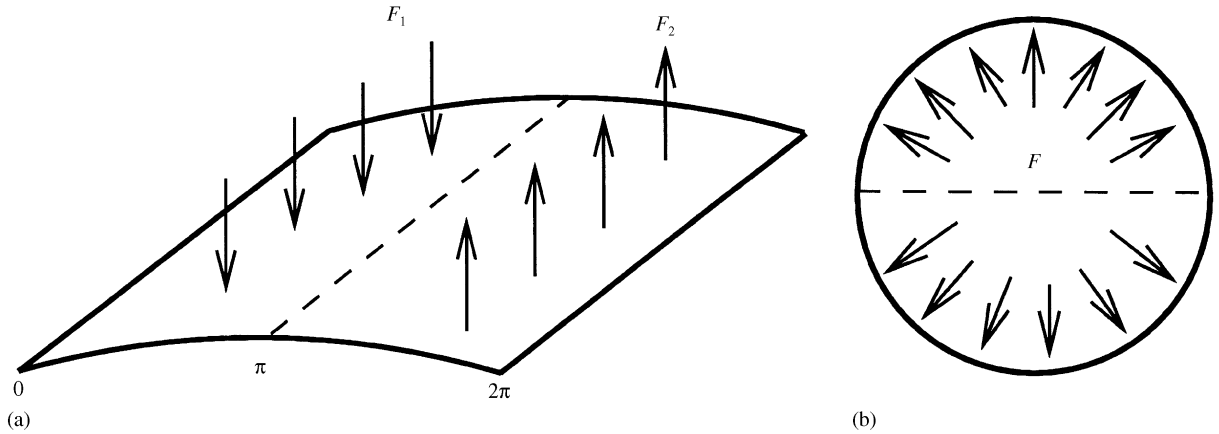

Fig. 8. (a) The external loading forces, F_1 and F_2, with the same magnitude but the opposite directions, for expanding the channel. (b) The crossection of the narrow channel in Fig. 8(b).

with the opposite directions. Hence, we design the external loading forces as

$$F = (f_x(r,t), f_y(r,t), f_z * (r,t))^{\mathrm{T}} = (\mathrm{sign}(\sin(t)), \mathrm{sign}(\sin(t)), 0)^{\mathrm{T}},$$

where

$$\mathrm{sign}(t) = \begin{cases} 1 & \text{if } t \geqslant 0, \\ -1 & \text{if } t < 0 \end{cases}$$

and the blending surfaces with an expanding channel are computed and drawn in Fig. 7(c). Other external loading forces are designed, to generate the blending surfaces in Fig. 7(d) and (e).

Besides Example 5.1, we have produced two more numerical examples: one is to blend the two perpendicular cylinders with different radii in Example 5.2 (see Fig. 9(a)–(c)), and the other is to blend a sphere and a cylinder in Example 5.3 (see Fig. 10(a)–(e)). Also the blending surfaces of Examples 5.2 and 5.3 are generated in the same way as Example 5.1, with the same parameters: $\mu = 0$, $P_c = 20$, $\sigma = 2$, $m = 8$ and $n = 4$ in the BP-FEM (3.12). Below we give the boundary displacement and tangent conditions.

Example 5.2.

$$\Delta^2 U = F,$$

$$\partial V_1 = \left(6\cos(t), 3\sqrt{3}\sin(t) - \sqrt{4^2 - \cos^2(t)}, \sqrt{3(4^2 - \cos^2(t))}\right)^{\mathrm{T}},$$

$$(\partial V_1)_n = \left(\frac{2\cos(t)\sqrt{16 - 9\cos^2(t)}}{\sin(t) - 3\sqrt{3}\cos^2(t)}, \frac{\sqrt{3}\sin(t)\sqrt{16 - 9\cos^2(t) - 6\cos^2(t)}}{\sin(t) - 3\sqrt{3}\cos^2(t)}, 1\right)^{\mathrm{T}},$$

$$\partial V_2 = (4\cos(t), 2\sqrt{3}\sin(t) - \tfrac{1}{2}r, 2\sin(t) + \tfrac{\sqrt{3}}{2}r)^{\mathrm{T}},$$

$$(\partial V_2)_n = (0, -\tfrac{1}{\sqrt{3}}, 1)^{\mathrm{T}},$$

where $t \in [0, 2\pi]$ and $r \in [8, 18]$.

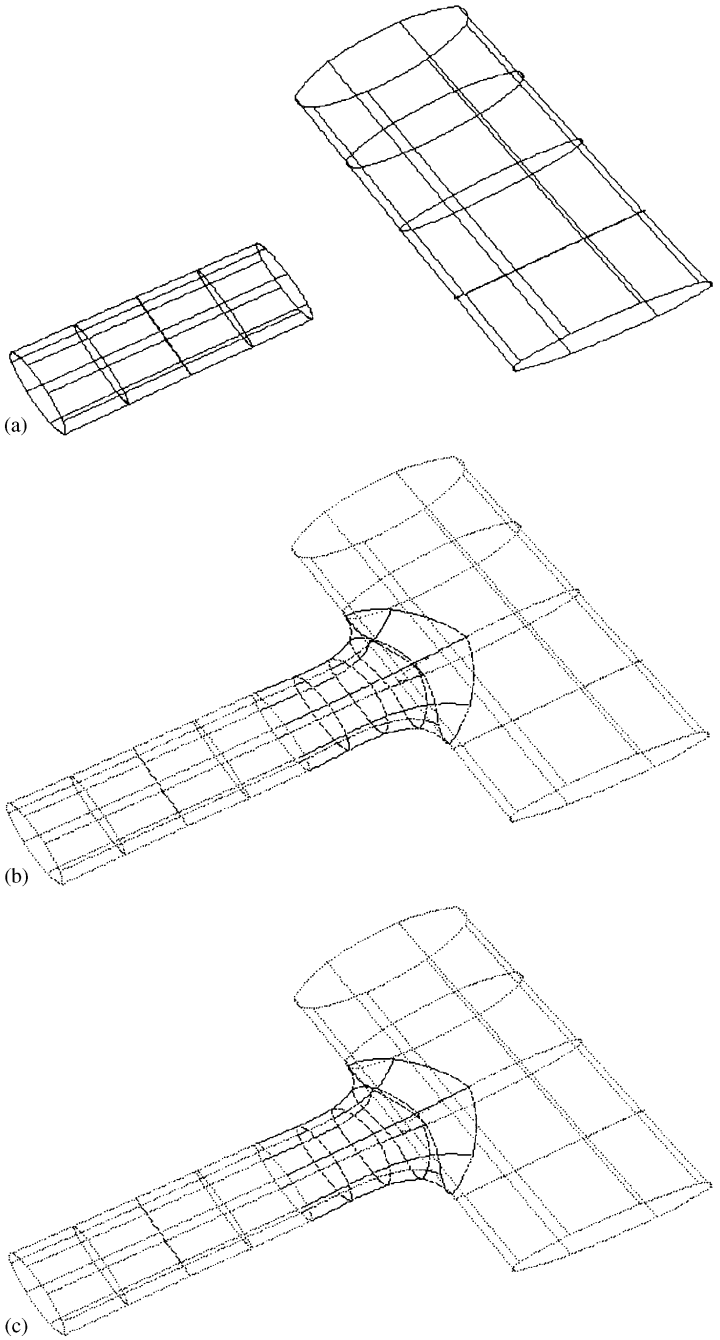

Fig. 9. (a) Two separated cylinders with different radii ($R=4$ and 8). (b) The blending surface by $F=(0,0,0)^{\mathrm{T}}$. (c) The blending surface by $F=(t^4\,\mathrm{sign}(\sin(t)),t^4\,\mathrm{sign}(\sin(t)),0)^{\mathrm{T}}$.

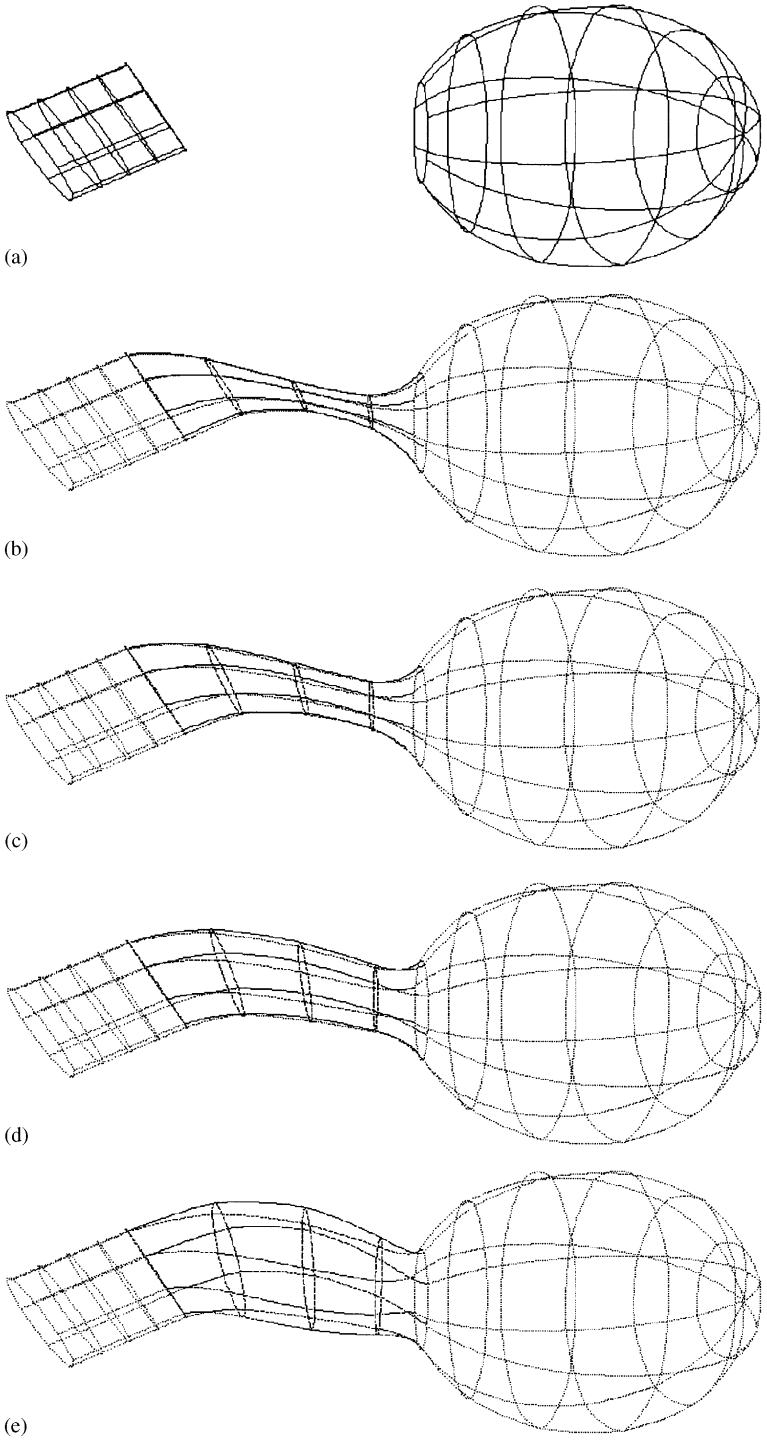

Fig. 10. (a) The cylinder with radius 5 and the sphere with radius 13. (b) The blending surface by $F = (0,0,0)^{\mathrm{T}}$. (c) The blending surface by $F = (t^4 \operatorname{sign}(\sin(t)), t^4 \operatorname{sign}(\sin(t)), 0)^{\mathrm{T}}$. (d) The blending surface by $F = (\sin(t)\operatorname{sign}(\sin(t)), \sin(t)\operatorname{sign}(\sin(t)), 0)^{\mathrm{T}}$. (e) The blending surface by $F = (\cos(t)\operatorname{sign}(\sin(t)), \cos(t)\operatorname{sign}(\sin(t)), 0)^{\mathrm{T}}$.

Example 5.3.

$$\Delta^2 U = F,$$

$$\partial V_1 = (5\cos(t), 5\sin(t), r)^{\mathrm{T}},$$

$$(\partial V_1)_n = \left(-\frac{12}{5}\cos(t), -\frac{12}{5}\sin(t), 1\right)^{\mathrm{T}},$$

$$\partial V_2 = \left(5\cos(t), \frac{5\sqrt{3}}{2}\sin(t) - \frac{r-37}{2}, \frac{5}{2}\sin(t) + \frac{\sqrt{3}(r-37)}{2} + 37\right)^{\mathrm{T}},$$

$$(\partial V_2)_n = (0, -\tfrac{1}{\sqrt{3}}, 1)^{\mathrm{T}},$$

$t \in [0, 2\pi]$ and $r \in [12, 32]$.

Note that the division numbers are only $m = 8$ and $n = 4$, and the resulted blending surfaces are satisfactory to engineering requirements. Double precision is good enough for practical application.

6. Extensions and remarks

The above discussions and algorithms can be easily extended to blending surfaces on linear constraints of displacements and tangent conditions on both interior and exterior boundaries. Many interesting applications of blending surfaces can be explored by following the ideas stated in [24] and this paper. Below we give only two samples.

Sample A: We consider more complicated joint conditions $\overline{BD}$ in Fig. 11, by relaxing the displacement conditions given before. Suppose that the righthand frame is a quadratic cone, and that the joint boundary is just located on the coordinate plane $x = \alpha$, where α is unknown (see Fig. 11). By our techniques, a suitable location $x = \alpha$, accompanied with the optimal blending surfaces in minimum energy, can be determined automatically.

Suppose that the left boundary conditions at $\overline{AC}$ are the same as in Section 2:

$$U|_{AC} = U_0, \qquad y_n = b_{10}x_n, \qquad z_n = b_{20}x_n \quad \text{on } \overline{AC}. \tag{6.1}$$

The quadratic cone is expressed as

$$y = a(x - x_0)\cos\theta\,; \qquad z = b(x - x_0)\sin\theta \quad \text{on } \overline{BD}, \tag{6.2}$$

where a, b and x_0 are given. If letting $\theta = 2\pi t$, the right displacement conditions and the tangent boundary conditions are written as

$$x = \alpha, \qquad y = a(\alpha - x_0)\cos(2\pi t), \qquad z = b(\alpha - x_0)\sin(2\pi t) \quad \text{on } \overline{BD} \tag{6.3}$$

and

$$y_n = a\cos(2\pi t)x_n, \qquad z_n = b\sin(2\pi t)x_n \quad \text{on } \overline{BD}. \tag{6.4}$$

The optimal location of plane $x = \alpha$ can also be obtained from the numerical algorithms similar to the BP-FEM.

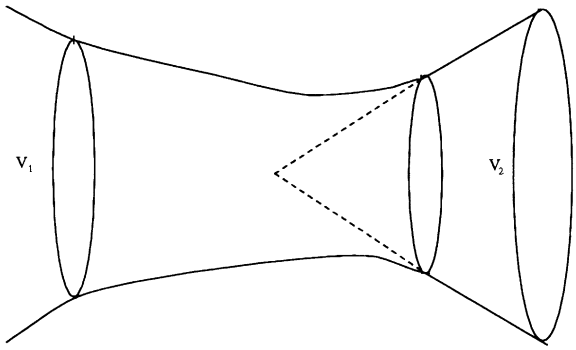

Fig. 11. A blending surface where ∂V_2 is a plane $x = \alpha$ with arbitrary α.

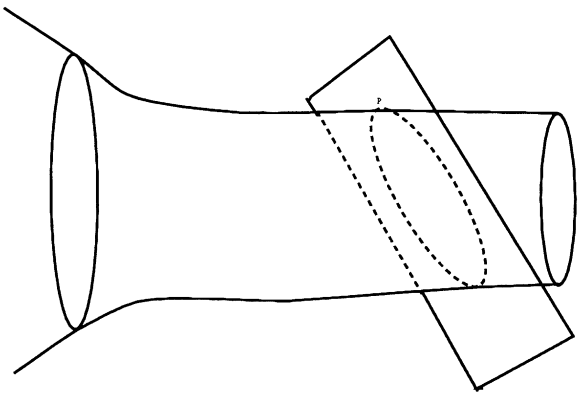

Fig. 12. A blending surface where ∂V_2 is an arbitrary plane passing by P.

Sample B: Suppose the right-hand frame is a cylinder along axis x, but a possible joint boundary is placed on an arbitrary plane just passing a given point P (see Fig. 12). Hence for the right boundary conditions, we should assign

$$a(x - x_P) + b(y - y_P) + c(z - z_P) = 0, \tag{6.5}$$

where a, b, c are unknown constants to be determined. We may then add the following penalty integral to the energy form (2.17):

$$\frac{P_c}{h^{2\sigma}} \int_{\overline{BD}} (a(x - x_P) + b(y - y_P) + c(z - z_P))^2 \, \mathrm{d}\ell. \tag{6.6}$$

After a suitable modification of definitions of spaces V_h and V_h^0, the optimal solutions with coefficients a, b and c can be obtained automatically, by following the approaches in Sections 2 and 3. All analytical conclusions may be carried our by following Section 4. For nonlinear boundary conditions, we may develop the corresponding BP-FEM as well.

7. Concluding remarks

1. In summary, the new approaches using PDEs are proposed in this paper, to construct general and complicated blending surfaces. The optimal blending surfaces are sought to minimize the global energy of the surface. The BP-FEMs are significant to treat complicated boundary conditions since algorithms can be carried out simply and easily, and since theoretical analysis is also provided. Based on the a posteriori interpolants of numerical solutions, not only may the superconvergence rates $O(h^3)$ and $O(h^{3.5})$ of second order of generalized derivatives over Ω be gained, but also the very high convergence rates $O(h^6)$ and $O(h^7)$ of the tangent and periodical boundary conditions of the solutions can be attained. Note that the analysis for superconvergence is made for $\mu \in [0, \frac{1}{2})$. In this paper we develop and apply the results of Lin and Yan [29] to the BP-FEM solutions involving complicated boundary conditions. Lemma 4.6 is basic and important, and the bounds in (4.35) and in Lemmas 4.8 and 4.9 are also new to [28,29].
2. Stability analysis is made for quasiuniform $\square_{ij}$ and $\mu \in [0, \frac{1}{2})$. The variable transformation (3.5) is also suggested to reduce significantly condition number of the associated matrix resulted. We derive its bounds as $O(h^{-4}) + O(h^{-1-2\sigma})$. It is due to high accuracy of the boundary constraints that h is chosen to be not necessarily small in practical applications, thus to save CPU time significantly, and to lessen the numerical instability.
3. More efforts are made in Section 5 to provide three interesting examples of real 3D blending surfaces, to show efficiency of the proposed techniques in the paper. In Chang [8], several techniques are introduced to evaluate the stiff matrices so that they may be double-checked to each other. Also the explicit and exact entries of stiff matrices are listed for users. Besides, from viewpoint of applications, functions F in (2.7) may be suitably chosen from the physical meanings and engineering requirements and numerical experiments, shown in Section 5.
4. The explicit algebraic function $z = f(x, y)$ in [26] can also serve as blending surface. However, when the blending boundary is curve on Γ_2; we should use the curved elements which is rather complicated. In this case, we may employ suitable parametric functions, to transfer the solution domain Ω into a rectangle, as done in this paper. This may greatly simplify numerical algorithms and programming. For the case when the left and right boundaries may be touched to the frame blending surfaces around corners (see Kosters (89)), the solution domain Ω should be chosen as a polygon. Triangular elements of Ciarlet (90) can be used; similar algorithms and analysis of BP-FEMs can also be carried out.
5. How to deal with the complicated boundary constraints is an important issue in blending surfaces. The ODE (ordinary differential equation) and numerical methods are also applied to the 3D blending curves, reported in other papers. Furthermore, the techniques described in this paper can also be employed to other kinds of linear and nonlinear boundary constraint conditions (see Samples A and B). Moreover, other kinds of coupling techniques described in Li [25] for interfaces may be employed to deal with the boundary constraints in blending surfaces as well. Again the merits of the algorithms in this paper lie in flexibility and generality to produce the blending surfaces satisfying the complicated boundary conditions. This paper and [24,26] provide a theoretical frame work of complicated blending surfaces of new trends.
6. Let us recall the study of blending surfaces in Parts I [24], II in [26] and III in this paper. In Part I we model the blending surfaces by the PDE solutions governed by the biharmonic equations, based on the physical intuition of resembling flexibly elastic thin plates, develop the BP-FEM to

handle the tangent and periodical boundary conditions, and derive optimal convergence rates for both interior solutions and boundary conditions. Note that the traditional techniques for blending surfaces are based on interpolations reported in numerous papers and many books; they suffer multiple solutions (see [16, p. 486]) and fail to deal with the complicated blending conditions in the modern engineering. This is a main motivation of our study. The PDE approaches will provide the unique blending solutions which are also optimal in minimum energy of the blending surfaces, and the BP-FEMs are well suited to treat the complicated boundary constraints. In this paper, we pursue superconvergence and stability for the BP-FEM and provide three real 3D samples of blending surfaces. The fidelity of the solutions to the boundary matching is our main concern; the new error bounds, convergence and superconvergence for the boundary conditions are studied and reported in Parts I–III. Indeed, Part II is a simple case of Parts I and III. Part II is also important, because the biharmonic solutions are of blending surfaces, because the analysis of the BP-FEM in convergence, superconvergence and stability is also significant to biharmonic equations, and because the simple exposition in Part II may help us reveal the ideas and spirits in Parts I and III much easier and readable. A remarkable consequence of study in Parts I–III is that the size of h of the finite elements in real computation may not be chosen small so that the double precision of computer may satisfy well the requirements by the moderate blending problems in engineering. On the whole, Parts I and II [24,26] and this paper combine theory and practice together for both biharmonic equations and blending surfaces, to form a systematic study on blending surfaces by PDEs and their numerical solutions.

Acknowledgements

We are grateful to Prof. Yan N.N. and the referee for their valuable suggestions to this manuscript.

References

[1] K.E. Atkinson, An Introduction to Numerical Analysis, 2nd Edition, Wiley, New York, 1989.
[2] I. Babuska, The finite element method with penalty, Math. Comput. 27 (1973) 221–228.
[3] C.L. Bajaj, I. Ihn, Algebraic surface design with Hermite interpolation, ACM Trans. Graphics 11 (1992) 61–91.
[4] J.W. Barret, C.M. Elliott, Finite element approximation of the Dirichlet problem using the boundary penalty method, Numer. Math. 49 (1986) 343–366.
[5] M.I.G. Bloor, M.J. Wilson, Generating blending surface using partial differential equations, CAD 21 (1989) 165–171.
[6] M.I.G. Bloor, M.J. Wilson, Using partial differential equations to generate free from surfaces, CAD 22 (1990) 202–212.
[7] G.F. Carey, T.T. Oden, Finite Elements, A Second Course, Vol. II, Prentice-Hall, Englewood Cliffs, NJ, 1983.
[8] C.S. Chang, Boundary penalty finite element method for blending surfaces, II. Superconvergence, stability and applications, Master Thesis, Department of Applied Mathematics, National Sun Yat-sen University, Kaohsiung, Taiwan, June 1998.
[9] B.K. Choi, Surface Modelling for CAD/CAM, Elsevier, Amsterdam, 1991.
[11] R. Courant, D. Hilbert, Methods of Mathematical Physics, Interscience Publishers, New York, 1953.
[12] P.J. Davis, P. Rabinowitz, Methods of Numerical integration, 2nd Edition, Academic Press Inc., San Diego, 1984.
[13] M. de Do, Carmo, Differential Geometry of Curves and Surfaces, Prentice-Hall, Englewood Cliffs, NJ, 1976.
[14] G. Farin, Curves and Surfaces for Computer Aided Geometric Design, A Practical Guide, 2nd Edition, Academic Press, New York, 1990.

[15] R.B. Fisher (Ed.), Design and Application of Curves and Surfaces, Oxford University Press, Oxford, 1994.
[16] J.D. Foley, A. van Dam, S.K. Feiner, J.F. Hughes, Computer Graphics, Principle and Practice, 2nd Edition, Addison–Wesley Publishing Company, Reading, MA, 1991.
[17] K. Fong, Z.C. Shi, Mathematical Theory on Elastic Structures, Science Publishing, Beijing, 1981 (in Chinese).
[18] J.A. Gregory (Ed.), The Mathematics of Surfaces, Clarendon Press, Oxford, 1986.
[19] C. Hoffmann, J. Hopcroft, Automatic surface generation in computer aided design, Visual Comput. 1 (1985) 92–100.
[20] J.J. Koenderink, Solid Shape, MIT Press, Cambridge, 1990.
[21] M. Kosters, Quadratic blending surfaces for corners, Visual Comput. 5 (1989) 134–146.
[22] Z.C. Li, On nonconforming combinations of various finite element methods for solving elliptic boundary value problems, SIAM J. Numer. Anal. 28 (1991) 446–475.
[23] Z.C. Li, Penalty-combined approaches to the Ritz-Galerkin and finite element methods for singularity problems of elliptic equations, Numer. Methods PDE 8 (1992) 33–57.
[24] Z.C. Li, Boundary penalty finite element methods for blending surfaces, I. Basic theory, J. Comput. Math. 16 (1998) 457–480.
[25] Z.C. Li, Combined Methods for Elliptic Equations with Singularities, Interfaces and Infinitives, Kluwer Academic Publishers, Boston, London, 1998.
[26] Z.C. Li, Boundary penalty finite element methods for blending surfaces, II. Biharmonic equations, J. Comput. Appl. Math. 110 (1999) 155–176.
[27] Q. Lin, Interpolated finite elements and global error recovery, Contemp. Math. 163 (1994) 93–109.
[28] Q. Lin, P. Luo, Global superconvergence of Hermite bicubic element for biharmonic equation, Beijing Math. 1 (Part 2) (1995) 52–64.
[29] Q. Lin, N.N. Yan, The Construction and Analysis of High Efficient FEM (in Chinese), Hobel University Publishing, Banding, China, 1996, pp. 54–67, 126–128.
[30] J.T. Marti, Introduction to Sobolev Spaces and Finite Element Solution of Elliptic Boundary Value Problems, Academic Press, London, 1986.
[31] A.W. Nutbourne, R.R. Martin, Differential Geometry Applied to Curves and Surface Design, Vol. I: Foundations, Wiley, New York, 1988.
[32] K. Ohkura, Y. Kakazu, Generalization of the potential method for blending three surfaces, CAD 24 (1992) 599–610.
[33] Z.C. Shi, On the convergence rate of the boundary penalty method, Int. J. Numer. Methods Eng. 20 (1984) 2027–2032.
[34] B.Q. Su, D.Y. Liu, Computational Geometry-Curve and Surface Modelling, Academic Press, Boston, 1989.
[35] M. Utku, D.F. Carey, Boundary penalty techniques, Comput Methods Appl. Mech. Eng. 39 (1982) 103–118.
[36] M. Utku, D.F. Carey, Penalty resolution of the Babuska circle paradox, Comput Methods Appl. Mech. Eng. 41 (1983) 11–28.
[37] J. Warren, Blending algebraic surfaces, ACM Trans. Graphics 8 (1989) 263–278.